NASA/TM-2011-217055

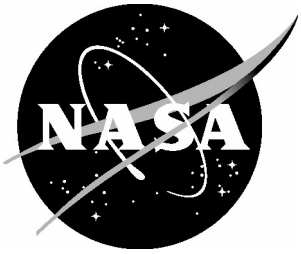

Entry, Descent and Landing Systems Analysis Study: Phase 2 Report on Exploration Feed-Forward Systems

Alicia M. Dwyer Ciancolo, Jody L. Davis, Walter C. Engelund, D. R. Komar, Eric M. Queen, Jamshid A. Samareh, David W. Way, and Thomas A. Zang
NASA Langley Research Center, Hampton, Virginia

Jeff G. Murch, Shawn A. Krizan, Aaron D. Olds, Richard W. Powell, and Jeremy D. Shidner
Analytical Mechanics Associates, Inc., Hampton, Virginia

David J. Kinney and M. Kathleen McGuire
NASA Ames Research Center, Moffett Field, California

James O. Arnold
University of California, Santa Cruz, California

M. Alan Covington
ERC, Inc., Edwards AFB, California

Ronald R. Sostaric and Carlie H. Zumwalt
NASA Johnson Space Center, Houston, Texas

Eduardo G. Llama
GBTech, Inc., Houston, Texas

February 2011

NASA STI Program . . . in Profile

Since its founding, NASA has been dedicated to the advancement of aeronautics and space science. The NASA scientific and technical information (STI) program plays a key part in helping NASA maintain this important role.

The NASA STI program operates under the auspices of the Agency Chief Information Officer. It collects, organizes, provides for archiving, and disseminates NASA's STI. The NASA STI program provides access to the NASA Aeronautics and Space Database and its public interface, the NASA Technical Report Server, thus providing one of the largest collections of aeronautical and space science STI in the world. Results are published in both non-NASA channels and by NASA in the NASA STI Report Series, which includes the following report types:

- TECHNICAL PUBLICATION. Reports of completed research or a major significant phase of research that present the results of NASA programs and include extensive data or theoretical analysis. Includes compilations of significant scientific and technical data and information deemed to be of continuing reference value. NASA counterpart of peer-reviewed formal professional papers, but having less stringent limitations on manuscript length and extent of graphic presentations.

- TECHNICAL MEMORANDUM. Scientific and technical findings that are preliminary or of specialized interest, e.g., quick release reports, working papers, and bibliographies that contain minimal annotation. Does not contain extensive analysis.

- CONTRACTOR REPORT. Scientific and technical findings by NASA-sponsored contractors and grantees.

- CONFERENCE PUBLICATION. Collected papers from scientific and technical conferences, symposia, seminars, or other meetings sponsored or co-sponsored by NASA.

- SPECIAL PUBLICATION. Scientific, technical, or historical information from NASA programs, projects, and missions, often concerned with subjects having substantial public interest.

- TECHNICAL TRANSLATION. English-language translations of foreign scientific and technical material pertinent to NASA's mission.

Specialized services also include creating custom thesauri, building customized databases, and organizing and publishing research results.

For more information about the NASA STI program, see the following:

- Access the NASA STI program home page at *http://www.sti.nasa.gov*

- E-mail your question via the Internet to help@sti.nasa.gov

- Fax your question to the NASA STI Help Desk at 443-757-5803

- Phone the NASA STI Help Desk at 443-757-5802

- Write to:
  NASA STI Help Desk
  NASA Center for AeroSpace Information
  7115 Standard Drive
  Hanover, MD 21076-1320

NASA/TM-2011-217055

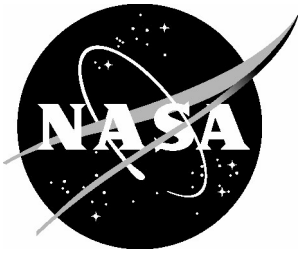

Entry, Descent and Landing Systems Analysis Study: Phase 2 Report on Exploration Feed-Forward Systems

Alicia M. Dwyer Ciancolo, Jody L. Davis, Walter C. Engelund, D. R. Komar, Eric M. Queen, Jamshid A. Samareh, David W. Way, and Thomas A. Zang
NASA Langley Research Center, Hampton, Virginia

Jeff G. Murch, Shawn A. Krizan, Aaron D. Olds, Richard W. Powell, and Jeremy D. Shidner
Analytical Mechanics Associates, Inc., Hampton, Virginia

David J. Kinney and M. Kathleen McGuire
NASA Ames Research Center, Moffett Field, California

James O. Arnold
University of California, Santa Cruz, California

M. Alan Covington
ERC, Inc., Edwards AFB, California

Ronald R. Sostaric and Carlie H. Zumwalt
NASA Johnson Space Center, Houston, Texas

Eduardo G. Llama
GBTech, Inc, Houston, Texas

National Aeronautics and
Space Administration

Langley Research Center
Hampton, Virginia 23681-2199

February 2011

Available from:

NASA Center for AeroSpace Information
7115 Standard Drive
Hanover, MD 21076-1320
443-757-5802

Table of Contents

List of Figures

List of Tables

Acronyms

ALHAT	Autonomous Landing and Hazard Avoidance Technology
Al-Li	Aluminum Lithium
APC	Analytic Predictor-Correction
ARMD	Aeronautics Research Mission Directorate
CCRB	Customer Content Review Board
CG	Center of Gravity
CH4	Methane
deg	degrees
deg/sec^2	degrees per second squared
DLV	Descent Landing Vehicle
DRA5	Design Reference Architecture 5.0
DRM	Design Reference Mission
EDL	Entry, Descent and Landing
EDL-SA	Entry, Descent and Landing Systems Analysis
EFF	Exploration Feed Forward
EKF	Extended Kalman Filter
ESMD	Exploration Systems Mission Directorate
ETDP	Exploration Technology Development Program
ETDD	Exploration Technology Development and Demonstration
EXAMINE	Exploration Architecture Model for IN-space and Earth-to-orbit
GR&A	Ground Rule and Assumption
HDA	Hazard Detection and Avoidance
HIAD	Hypersonic Inflatable Aerodynamic Decelerator
HYPAS	Hybrid Predictor-Corrector Aerocapture Scheme
IAD	Inflatable Aerodynamic Decelerator
IMU	Inertial Measurement Unit
IRVE	Inflatable Re-entry Vehicle
Isp	Specific Impulse
ISRU	In-situ Resource Utilization
kg	kilograms
kg/m^2	kilograms per square meter
km	kilometers

kN	kilo Newtons
kW	kilo Watt
lbf	pounds of force
LCH4	Liquid Methane
LOX	Liquid Oxygen
LQR	Linear Quadratic Regulator
L/D	Lift-to-Drag Ratio
m	meters
m/s	meters/second
MGA	Mass Growth Allowance
MLI	Multilayer Insulation
MMH	monomethylhydrazine
MOLA	Mars Orbiter Laser Altimeter
MPS	Main Propulsion System
MSL	Mars Science Laboratory
t	metric ton
NPC	Numerical Predictor-Corrector
NTO	nitrogen tetroxide
OCE	Office of the Chief Engineer
PICA	Phenolic Impregnated Carbon Ablato*r*
PID	Proportional Integral Derivative
RCS	Reaction Control System
RSE	Response Surface Equation
s	seconds
SI	Shape Integral
SMD	Science Mission Directorate
SRP	Supersonic Retro-propulsion
TDP	Technology Development Project
TISC	Technology Investment Steering Committee
TPS	Thermal Protection System
TRL	Technology Readiness Level
TRN	Terrain Relative Navigation
T/W	Thrust-to-Weight Ratio
ΔV	change in velocity

Acknowledgements

In addition to the authors of this report, other individuals have contributed in some way to the Exploration Feed Forward Study. The HIAD insulative TPS mass model was provided by Joseph Del Corso, Stephen J. Hughes and F. McNeil Cheatwood. Useful comments on the HIAD TPS mass models were given by Kamran Daryabeigi. The details on the Movable Fission Power System payload were furnished by Lee E. Mason. The EDL-SA assessment of ALHAT technology at Mars benefited from the input of the ETDD ALHAT Team (Chirold D. Epp and Edward Robertson). Furthermore, the work reported in this paper benefited greatly from all those who contributed to the first year of the EDL-SA Study.

Feedback on the draft Design Reference Missions, Ground Rules and Assumption, and the Evaluation Criteria was provided by Bret C. Drake, Dana C. Gould, and Charles M. Lundquist. The Internal Peer Review Panel (Anthony M. Calomino, Charles H. Campbell, Christopher J. Cerimele, Karl T. Edquist, Chirold D. Epp, Mark M Hammerschmidt, Stephen J. Hughes, Mark D. Rezin and Michael J. Wright) provided valuable comments.

The team is appreciative of the efforts of Farhad Tahmasabi and Harold M. Bell of the Office of the Chief Engineer for their guidance and support, and especially for the efforts of our sponsor, Mike Ryschkewitsch, the NASA Chief Engineer. Finally, the EDL Systems Analysis Study was only possible because of the persistent and effective advocacy of Walter C. Engelund and Stephen P. Sandford.

Abstract

NASA senior management commissioned the Entry, Descent and Landing Systems Analysis (EDL-SA) Study in 2008 to identify and roadmap the Entry, Descent and Landing (EDL) technology investments that the agency needed to successfully land large payloads at Mars for both robotic and human-scale missions. Year 1 of the study focused on technologies required for Exploration-class missions to land payloads of 10 to 50 t. Inflatable decelerators, rigid aeroshell and supersonic retro-propulsion emerged as the top candidate technologies. In Year 2 of the study, low TRL technologies identified in Year 1, inflatables aeroshells and supersonic retropropulsion, were combined to create a demonstration precursor robotic mission. This part of the EDL-SA Year 2 effort, called Exploration Feed Forward (EFF), took much of the systems analysis simulation and component model development from Year 1 to the next level of detail.

A main objective of the study was to determine the maximum payload mass capability of a Delta IV-H launch vehicle (launch mass of 7.2 t) for the 2024 Mars opportunity. The simulation results, using the latest component mass models, indicated that a direct entry system could deliver approximately 3.5 t to 0 km above the Mars Orbiter Laser Altimeter (MOLA) areoid. A second objective was to characterize the performance required of the supersonic retro-propulsion system. The study, which assumed four engines with a specific impulse of 338s and a system thrust-to-weight of 3.7 Mars g's, yielded descent engine initiation between Mach 1.4 and 1.8 at an altitude between 3 and 8 km. A third major objective was to use the high fidelity entry simulation to characterize an Autonomous Landing and Hazard Avoidance Technology (ALHAT) like sensor suite for Mars. Initial performance range results were obtained for terrain relative navigation, hazard detection and avoidance, velocimeter and altimeter sensor systems.

This document provides a summary of the analysis performed to meet the EFF objectives and provides recommendations, based on the results, for future investment.

1 Executive Summary

The Exploration-class missions studied in the first year of the Entry, Descent and Landing Systems Analysis (EDL-SA) [1] effort identified technologies required to land cargo or crewed missions requiring payloads between 10 and 50 t on Mars. The technology areas included the rigid aeroshell from the Mars Design Reference Architecture 5.0 (DRA5) [2], inflatable aerodynamic decelerators and supersonic retropropulsion. Candidate technology areas were assessed against a set of eight "EDL Architectures", i.e., representative architectures (high-level designs) against which the benefits of the technology areas were evaluated. As a result of the study, two technology areas that presented substantial potential for high mass to the surface—hypersonic inflatable aerodynamic accelerators (HIADs) and supersonic retropropulsion (SRP)—were combined to create a robotic precursor demonstration mission for detailed evaluation in the EDL-SA Year 2 effort.

The precursor demonstration mission of Year 2 is referred to as Exploration Feed Forward (EFF). The Design Reference Mission (DRM), Ground Rules & Assumptions (GR&As) and Evaluation criteria (see Appendix A) for the study were approved by the managers of the ARMD, ESMD and SMD technology programs in June 2010, prior to the execution of the simulation and evaluation of results.

The EFF baseline mission includes a conceptual 2 t nuclear power source payload that is aerocaptured into a 500 km circular orbit at Mars using a 14 m HIAD. Following aerocapture the 14 m HIAD is jettisoned and an 8 m entry HIAD is inflated. The vehicle has a nominal Lift-to-Drag (L/D) ratio equal to 0.25 and is guided. At approximately Mach 2 the entry HIAD is jettisoned and supersonic retropropulsion is initiated. The mission terminates with a touchdown velocity of 1 m/s at 0 km above the MOLA areoid.

The goals of EFF, evaluated using the single architecture described above, included the following.

1. Determine the maximum payload delivery capability of a Delta IV-H
2. Determine required performance of supersonic retropropulsion
3. Increase the level of fidelity of all models
4. Determine optimal materials, L/D and HIAD size for aerocapture and entry
5. Determine if center of gravity control provides benefits over bank control for the HIAD
6. Determine sensor performance for an ALHAT system at Mars.

Under the assumptions made for EFF, the maximum deliverable payload of a Delta IV-H is approximately 3.5 t (Sect 3). Simulation results indicate that SRP performance for a mission of this class, assuming 4 engines with a specific impulse of 338 s and a thrust to weight of 3.7 Mars g's, requires engine initiation between Mach 1.4 and 1.8 at altitudes between 3 and 8 km (Sect 5.1). Using models of TPS materials currently being developed by the Inflatable Re-entry Vehicle 3 (IRVE-3) and the Entry, Descent and Landing Technology Development Project (EDL TDP), analysis shows that TPS materials maturation is required, but that the materials appear feasible for the application considered (Sect. 4). Performance of ALHAT like sensors for Mars is assessed for a system that excluded terrain relative navigation. The initial sensor results were provided to the ALHAT project (Sect 5). Details of the EFF packaging (Sect. 3) indicate that the configuration may require a redesign to eliminate or account for the risk of heating due to flow recircularization behind the HIADs. Schedule and funding constraints limited the HIAD controllability assessment to a more detailed assessment of the bank controller used in the Year 1 Exploration-class missions; however the analysis did evaluate the effects of additional guidance options (Sect. 4).

The primary technology recommendations that resulted from the EFF work are listed in Table 1 and are intended to complement the recommendations of EDL-SA Year 1 Exploration-class analysis. The

combined technology recommendations from Years 1 and 2 are provided in Appendix B. Also an internal peer review was conducted Dec. 1-2, 2010. The feedback received was extremely beneficial and is documented [3] elsewhere.

Table 1. TDP EFF Recommenations

Technology Area	TDP Content
Rigid Aeroshell	(1) Though not considered here, new knowledge of potential Mars payloads (being half the length considered for DRA5[2]) suggest that size shape and mass optimization is needed. (2) Transition maneuvers need to be fully examined (3) Software configuration of system analysis studies is essential
Supersonic Retro-Propulsion	**Recommend to accelerate SRP development to a point that feasibility has been demonstrated ASAP**
Deployable/Inflatable Decelerators	(1) Consider size, shape and mass optimization, effect of charring, and alternate modes of guidance and control and transitions. (2) Consider rigid deployables not considered above (3) Utilize software configuration control mechanisms in systems analysis studies
GN&C	Additional insight into performance requirements was gained, but no fundamentally new objectives were identified
Aerocapture Development	(1) Consider ability to jettison drag device after aerocapture pass but while in sensible atmosphere (2) Investigate torques caused by aero/RCS interactions (3) Double aerodynamic uncertainties in systems analysis
Supersonic Retro-Propulsion & Deployable/Inflatable Decelerator Flight Test Program	Consider developing a dedicated reusable testbed to test critical EDL technologies and flight instrumentation
Aerocapture Flight Test	Remains a high priority
Feed-Forward Technology Mars Flight Test	Flight demonstration (TRL=8) of EFF technologies at Mars with real payload; Use technologies from EDL-SA (or future studies) EFF robotic mission design as baseline

2 Exploration Feed Forward Methodology

The design methodology used for the EFF study is based on lessons learned from both DRA5 [2] and the EDL-SA Year 1 Exploration-class study [1] and recent developments in several technology areas. Primary technology recommendations from the EDL-SA Exploration study included HIADs, rigid aeroshells and supersonic retropropulsion. Since the conclusion of the Year 1 study, development has continued in NASA technology programs on the IRVE inflatable concept (ARMD). In addition, testing of both ablator (ESMD) and insulator (ARMD) materials has demonstrated TPS feasibility. The continued development has led to an increase in maturity in inflatable aeroshell technology and suggests that inflatables should continue to be considered for exploration missions due to the potential for large arrival mass reductions or significant payload fraction increases. The development of ALHAT sensors for lunar missions has prompted the desire for detailed simulation analysis of a similar system for Mars missions. Also, recent packaging arrangements for the Exploration-class mission payloads indicate that the 10 x 30 m aeroshell considered in DRA5 and EDL-SA Year 1 may be too long by a factor or two. Another concern recognized in the EDL-SA Exploration study was the lack in understanding the ability to control large HIADs during aerocapture and entry. These, coupled with the desire to ascertain details of the next level of exploration system design, encompass the motivation for the architecture considered for EFF.

Resources available for the EDL-SA Year 2 EFF work necessitated the selection of a single architecture class that would enable analysis of the maximum number of feed forward technologies. The baseline architecture, EFF-1, shown in Figure 1, considers a Dual HIAD system, (14 m HIAD for aerocapture and 8 m HIAD for entry; sizes were optimized to maximize landed payload mass), supersonic retropropulsion, a Movable Fission Power System candidate payload [4] (see Figure 2) and an ALHAT sensor suite. EFF assumed a maximum launch mass capability of a Delta IV-H (7.2 t) and an arrival velocity at Mars of 7.3 km/s., consistent with the 2024 opportunity chosen for the DRM. Other mission assumptions can be found in Appendix A. Variations of this baseline were considered to examine the impact on landed payload. EFF-2 considers the use of a single HIAD sized for both aerocapture and entry, and EFF-3 and 4 consider HIADs sized for a direct entry of 7.3 (2024 “worse case” opportunity) and 5.8 (MSL like) km/s respectively. All EFF configurations are shown in Figure 1.

Fidelity of the POST2 simulation from Year 1, as well as many of the models (goal #3 in Sect 1) increased significantly over exploration work in EDL-SA Year 1. The model upgrades required the simulation to upgrade from 3 Degrees of Freedom (DOF) to 6DOF. Identifying a defined payload allowed for an estimation of vehicle mass properties including inertias. The 6DOF aerocapture simulation allowed for analysis of vehicle performance using several guidance and control algorithms. The 6DOF entry simulation allowed for sensor performance analysis of the ALHAT like sensor suite and provided environmental characteristics for a SRP system.

The initial intent was to optimize the 6DOF aerocapture and 6DOF entry simulations using the lightest mass model derived from technology program input. Next, using the closed EFF-1 system, perform the HIAD controllability analysis using multiple controllers and guidance algorithms on the aerocapture configuration. Then, using the selected optimal guidance/controller combination, compare the landed mass capability by evaluating the mass savings of a single HIAD (EFF-2) and direct entry (EFF-3 &4). Finally the ALHAT assessment would be performed on the configuration that landed the maximum payload. However, a major ***lesson learned*** in EFF, is that detailed model development takes time that the EFF project was not able to accommodate. Therefore, a slightly revised approach was taken that allowed the decoupling of the three major assessments -- optimum landed mass (Sect 3), the HIAD controllability (Sect 4) and the ALHAT sensor performance (Sect 5). The details of the approach and analysis performed for each assessment is described in the following sections. Each section also summarizes the technology recommendations, other lessons learned, and proposed work for future Exploration-class system analysis studies.

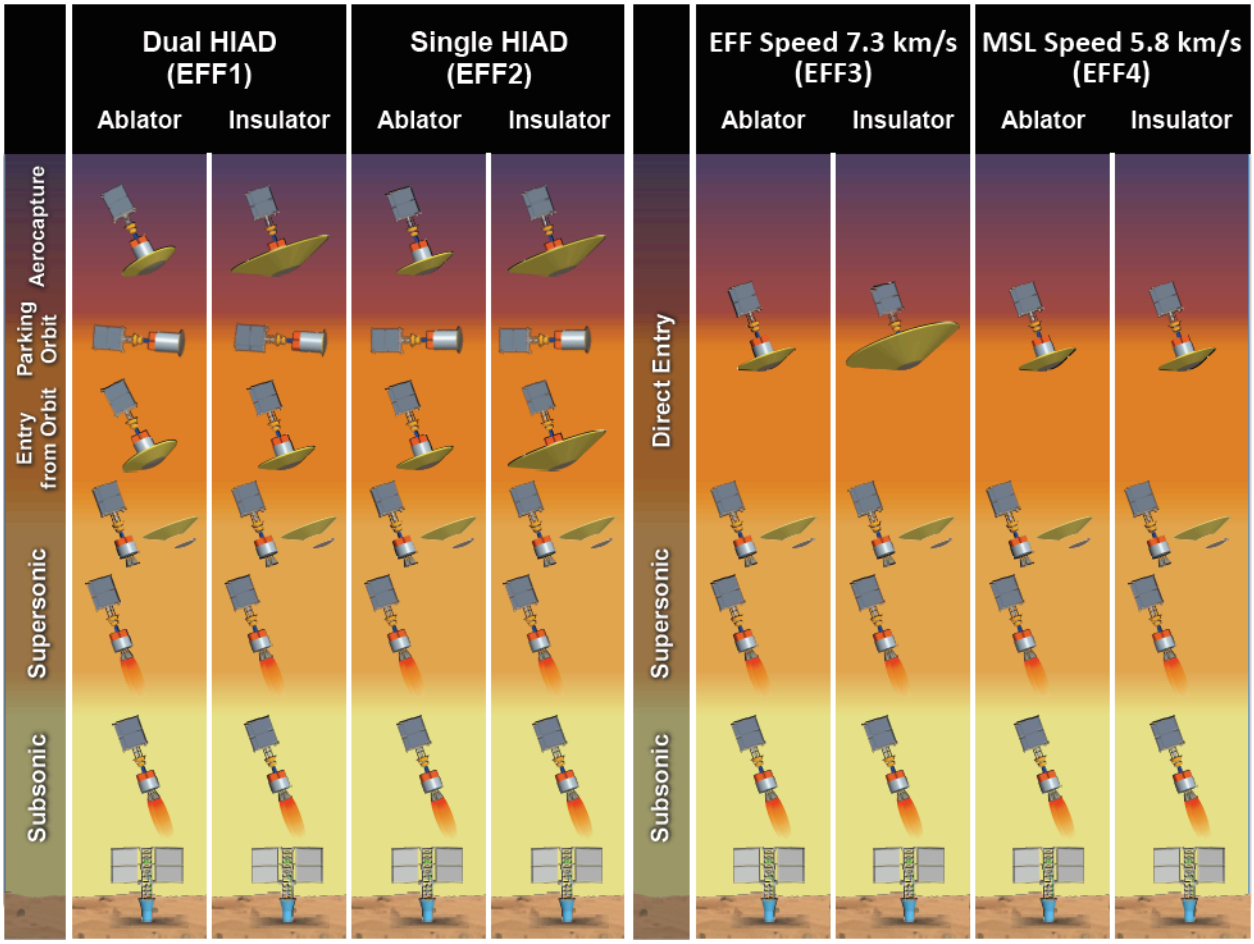

Figure 1. EFF Architectures

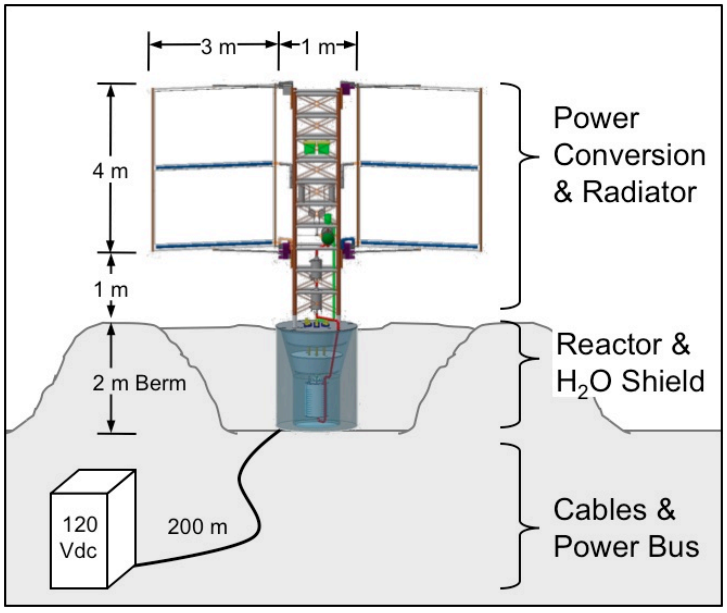

Figure 2. Movable Fission Power System Concept [4]

3 Landed Mass Assessment

The landed mass assessment required an update to mass models used in the EDL-SA Exploration-class study, which assumed a 40 t payload. A ***lesson learned*** from Year 1 was that parametric models allow for much easier design optimization and trade studies. Therefore, EFF followed an approach to perform simultaneous vehicle sizing and mission design for all four architectures. The approach requires a parametric mass model that mathematically represents mass components as a function of vehicle dimensions and key mission environmental parameters such as maximum dynamic pressures and total heat load.

The four architectures shown in Figure 1 share three major mass components: payload, Hypersonic Inflatable Aerodynamic Decelerator (HIAD), and descent landing vehicle (DLV). Figure 3 shows the overall process used to develop the required parametric mass models. A Java and Python based mass estimating tool was developed to approximate mass for inflatable elements of HIADs. This tool was used to generate masses for a large number of HIAD diameters, and these approximate masses were fitted with response surface equations (RSE). Technology programs provided two TPS mass models -- an ablator (from EDL TDP) and an insulator material (from IRVE). These were provided as a set of tables and simple analytical equations. An RSE was also used to model DLV mass. The RSEs, tables, and simple equations were combined into a set of C routines with additional equations for other mass components (e.g., rigid heatshield). The resulting C routines were integrated into POST2 for vehicle sizing and mission design. This process was similar to the approach used for Year 1 [1]. A margin of 49.5% was applied across all mass components including TPS. The next subsections include detailed discussion on the payload, HIAD, and TPS mass models. The last subsection concludes with a list of mass modeling specific recommendations for future enhancements.

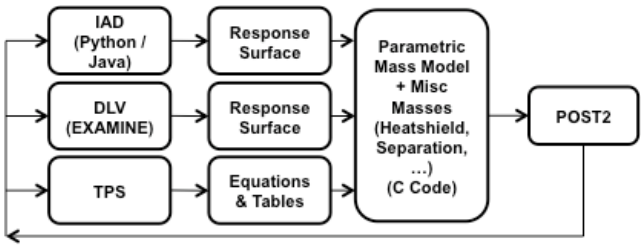

Figure 3. Mass Model Process

3.1 Payload

The candidate payload for this study was a small Movable Fission Power System (MFPS) [4] shown in Figure 2. The power plant mass is 1615 kg, and the mass for power management and distribution system is 415 kg, yielding a target landed payload of approximately 2 t. There are two options for payload surface mobility: 1) attach the payload to a rover that will act as a mobile platform for the power plant, and 2) pre-deploy a rover and a crane that will move the power plant to the operating site. Neither of these two mobility options was included in the current study, although there appears to be sufficient landed payload capability to include them with the MFPS on a single lander. Analysis was done to determine the payload's mass properties as defined in Ref [4]. The values were used in the HIAD controllability and ALHAT 6DOF analyses. However, mass modeling simulation considered only 3DOF trajectories to determine maximum landed mass and did not rescale the payload mass properties according to landed payload capability greater than 2 t. The impact of the change in the mass properties to accommodate larger vehicle was not evaluated. However, the controller was designed to generated pure accelerations and did not define thruster size, location or orientation. Therefore the 6DOF analysis could be performed independent of the payload mass properties.

It was also recognized that the payload configuration presented in Ref [4] might not be optimal for the entry configuration (HIAD + SRP) selected for the study. Options to shorten the payload were considered but the team elected to use the payload as defined and impose constraints on the diameter of the HIAD

and the angle of attack to mitigate flow impingement issues that may result from the long payload.

3.2 Hypersonic Inflatable Aerodynamic Decelerator (HIAD)

The HIAD model is a 65° sphere cone aeroshell that includes an inflatable decelerator, flexible TPS, separation mechanism, payload adapter, and a rigid spherical cap. The mass of the inflatable decelerator is based on the models developed by NASA in the 1960's and 1970's. The inflatable decelerator is identical to that used in the Year 1 study and is described in detail in the TM [1] and the AIAA paper on the mass model [5]. However, based on analysis and ***lessons learned*** in Year 1, the angle was changed from a 60° to a 65° sphere cone to reduce heating while maintaining acceptable performance.

3.3 Thermal Protection System Trade

The aerothermal environments used in this study were developed using the same methodology and margins that were employed in the year 1 Exploration study [1]. Additional detail on the methodology is provided in [6].

The thermal protection system (TPS) is one of the key components of HIAD aeroshells; it protects the inflatable decelerator from the extreme thermal environment during the aerocapture and entry phases. The HIAD TPS must be lightweight, suitable for efficient packaging and be capable of performing its function upon deployment after being stowed for periods of up to 6 months. Ablator and insulator concepts are currently two primary candidates for the HIAD TPS. The ablator mass model used in this study was developed at NASA Ames Research Center, and it was based on SIRCA-flex (flexible Q-felt plus silicone matrix) and PICA-flex (flexible Q-felt plus phenolic matrix)) concepts [6,7]. The insulator mass model was developed at NASA Langley Research Center, and it was based on a multilayer concept with an outer fabric (Nextel 440), an insulator (Pyrogel 3350), and a laminated gas barrier (Kapton-Kevlar-Kapton layer). The model, based on the IRVE 3 and 4 concepts, does have manufacturability, packaging and development maturity.

The ablator TPS concept has a higher areal density than that of the insulator, but can operate in environments with higher heat rates (up to 115 W/cm^2 for SIRCA-flex and up to 450 W/cm^2 for PICA-flex [7]). Insulators are currently limited to peak heat rates of ~60 W/cm^2. The optimal diameter for ablator and insulator HIADs are different: ablators tend to be more mass efficient for smaller diameter HIADs, while the insulators are more mass efficient for larger diameters HIADs.

A diameter sweep trade study was performed to identify optimal diameters and resulting payloads for both ablator and insulator TPS concepts under the constraint that the HIAD diameter remain large enough to prevent shear layer impingement on the payload. Figure C-19 to C-21 in Appendix C show details of the trade study, and Table 2 shows the trade study summary. The maximum available payload varies between 2.6-3.6 t, depending on the architecture, the TPS concept, and the arrival velocity. Based on the EFF assumptions, the ablator concept can generally deliver larger payloads compared to the insulator model. While the delivered masses with the two TPS systems are comparable, the HIADs using ablator TPS have considerably smaller diameters, as expected. Specifically, this study suggests that a single, dual heat pulse, 8 meter HIAD with ablator TPS can deliver the largest payload for missions using aerocapture, while the largest mass delivered for a direct entry configuration (5.8 km/s) uses an 8 meter HIAD with insulator TPS. The mass penalty for aerocapture must be traded with the increased flexibility to mission and entry timeline. Using aerocapture, the vehicle can wait in the target orbit until all subsystems are checked out and environmental conditions are ideal for entry.

As shown in Appendix C Figs. C-19-f, C-20-f, and C-21-f, the maximum available payload delivery is a strong function of TPS maximum operating heat rate; TPS concepts with higher maximum operating heat rate can deliver larger payloads. Since the current study considered HIADS of diameters that

prevented flow impingement on the payload, SIRCA-flex was adequate for the ablative TPS. PICA-flex would be suitable for smaller diameter HIADs with the corresponding increased peak heating.

Table 2. Results of the HIAD Diameter Mass Trade

			EFF-1 Dual HIAD		EFF-2 Single HIAD			EFF-3 Direct Entry, 7.2 km/s		EFF-4 Direct Entry, 5.8 km/s	
	Units		Ablator	Insulator	Ablator	Insulator		Ablator	Insulator	Ablator	Insulator
Maximum Payload	kg	Aerocapture	**2627**	**2371**	**2881**	**2589**	Direct Entry	**3294**	**2953**	**3442**	**3584**
Diameter	m		8	14	8	14		8	16	8	8
Max Dynamic Pressure	Pa		4259	1464	4259	1464		5922	2017	5791	2781
Inflatable Mass	kg		85	204				113	395	111	60
Max Heat Rate	W/cm2		108.7	44.5	108.6	44.5		111	48	67	49
Heat Load	MJ/m2		109	44	109	44		80	26	41	51
TPS Mass	kg		347	524				367	685	304	183
Rigid Diameter	m		4.3	4.3	4.3	4.3		4.3	4.3	4.3	4.3
Rigid Heatshield Mass	kg		91	91				91	91	91	91
Payload Adaptor Mass	kg		71	71				71	71	71	71
Separation Mass	kg		58	66				59	76	58	53
Diameter	m	Entry	8	8	8	14					
Max Dynamic Pressure	Pa		1248	1147	1460	500					
Inflatable Mass	kg		40	38	85	204					
Max Heat Rate	W/cm2		5.0	4.5	5	2					
Heat Load	MJ/m2		14.8	15.1	17	8					
TPS Mass	kg		198	165	417	744					
Rigid Diameter	m		3.6	3.6							
Rigid Heatshield Mass	kg		64	64	91	91					
Payload Adaptor Mass	kg		64	61	71	71					
Separation Mass	kg		45	44	60	72					

A sensitivity analysis was performed for TPS areal density. The results are shown in Table 3. A 25% increase in TPS areal density would result in 1.4 to 8.7% reduction in the maximum available payload.

Table 3. Sensitivity Analysis for TPS Areal Density

		Ablator		Insulator	
		Baseline	Baseline TPS + 25% Increase in TPS Areal Density	Baseline	Baseline TPS + 25% Increase in TPS Areal Density
EFF-1 Dual HIAD	AC TPS Mass, kg	347	433	524	655
	Entry TPS Mass, kg	198	244	165	206
	Payload, t	**2.63**	2.48	2.37	2.18
	Payload Reduction, %		-5.6%		-7.9%
	Payload/Launch Mass	0.36	0.34	0.33	0.30
EFF-2 Single HIAD	TPS Mass, kg	417	522	744	930
	Payload, t	**2.88**	2.76	2.59	2.36
	Payload Reduction, %		-4.2%		-8.7%
	Payload/Launch Mass	0.40	0.38	0.36	0.33
EFF-3 Direct Entry	TPS Mass, kg	367	460	685	855
	Payload, t	**3.29**	3.19	2.95	2.76
	Payload Reduction, %		-3.2%		-6.7%
	Payload/Launch Mass	0.46	0.44	0.41	0.38
EFF-4 Direct Entry	TPS Mass, kg	304	380	183	230
	Payload, t	3.44	3.35	**3.58**	3.53
	Payload Reduction, %		-2.5%		-1.4%
	Payload/Launch Mass	0.48	0.47	0.50	0.49

3.4 Descent Stage

This section presents the approach used in EFF to establish an integrated mass model and to summarize the ground rules and assumptions used to size the SRP, herein referred to as the descent stage.

The Exploration Architecture Model for IN-space and Earth-to-orbit (EXAMINE) [8] modeling framework, developed at NASA Langley Research Center, was used to model the mission events for each EFF configuration, develop the parametric mass estimates of the descent stage for all architectures, and to generate a mass model of the integrated system for use in the trajectory analysis. A methodology utilizing RSEs was employed for this effort to increase analytical efficiency and utility by enabling the following:

- Eliminating manual trajectory-sizing iterations;
- Enabling mass closure within the trajectory optimization framework;
- Enabling optimization of system configuration and element sizing variables in conjunction with trajectory optimization.

The primary descent stage structure is a 2.6 m diameter aluminum-lithium (Al-Li) cylinder that supports the tank system and payload. Thrust structure mass is based on a historical fit accounting for stage diameter, the number of engines and the thrust load. Secondary structure mass is 5% of the primary plus thrust structure masses. Landing gear mass is 2.5% of the landed mass on Mars. Multilayer insulation (MLI) is 5 cm thick (39.4 kg/m3) covering the exterior structure, providing thermal control of the spacecraft. During trans-Mars coast, a 3-junction gallium-arsenide photovoltaic array that provides 0.5 kilowatts (kW) of power for the EFF spacecraft. During entry and landing, two lithium-ion batteries each provide 1 kW for 2 hours of operation with 100% depth of discharge. Power is managed and distributed with a 115 volt alternating current system sized to handle 1 kW peak power at 90% efficiency. Waste heat (up to 1 kW) is collected from coldplates using an ammonia fluid loop and rejected using a body-mounted radiator. Avionics, including command, control and data handling, communication, guidance, navigation and control (GN&C), and instrumentation, are derived from MSL.

For the EFF study, the goal is to determine the maximum deliverable payload (~2-4 t) to the surface using a descent stage that provides retro-propulsion for supersonic, subsonic and terminal descent and landing. The model used for EDL-SA Year 1, which landed 40 t, was not well suited for this purpose. For a better comparison, EFF followed Mars Science Laboratory (MSL) in using a descent stage that employs a pressure-fed mono-propellant hydrazine propulsion system (with a specific impulse of less than 240 seconds [9]) to provide retro-propulsion for powered subsonic descent, sky crane, and flyaway maneuvers that deliver a payload to Mars' surface that is less than one metric ton. Since the landed payload requirement and descent stage functionality (in terms of propulsive delta-V) required are greater for EFF relative to MSL, a higher performing propulsion system is needed given that the total mass delivered to trans-Mars insertion is limited to 7.2 metric tons by the Delta IV-H launch vehicle capability [10]. Thus, a *pressure-fed* engine burning nitrogen tetroxide (NTO) and monomethylhydrazine (MMH) propellants was initially selected for EFF due to its increased vacuum specific impulse (Isp) compared to the mono-propellant hydrazine. However, preliminary analysis using this pressure-fed engine indicated that the maximum payload delivery capability from the closure analysis would be less than desired. A trade study was then performed to evaluate the payload performance improvement of both a pump-fed NTO/MMH system and a pump-fed engine using liquid oxygen (LOX) and liquid methane (LCH4) propellants. This study assumed the same payload and delta-V for each option and total descent stage wet mass was used to evaluate performance relative to the pressure-fed NTO/MMH case.

As shown in Figure 4, the pump-fed NTO/MMH stage mass decreased (relative to the pressure-fed NTO/MMH case) about 500 kg as both dry mass and propellant mass required decreased due to the

increased Isp. The pump-fed LOX/CH4 stage mass also decreased relative to the pressure-fed NTO/MMH stage, but not as much as the pump-fed NTO/MMH case. This is because the low density of the cryogenic methane fuel requires more dry mass (larger tanks and more structure to support the tankage, increased tank thermal control) and the inert mass is increased relative to the storable options due to the boiloff of the cryogenic propellants during the interplanetary coast.

Based on these results, a *pump-fed* NTO/MMH engine system was selected for EFF. Note that selection of this system was based purely on performance potential. Two key issues related to risk need to be considered further:

Mission risk associated with starting four pump-fed engines (utilizing a gas generator cycle) for the supersonic retro-propulsion maneuver following the 4-6 month interplanetary coast from Earth to Mars.

Development risk to enable deep throttling of the pump-fed engine to support landing: four engines operating together require throttling to 20% power level for landing while two engines operating together (with two shutdown) require throttling to 40% power level.

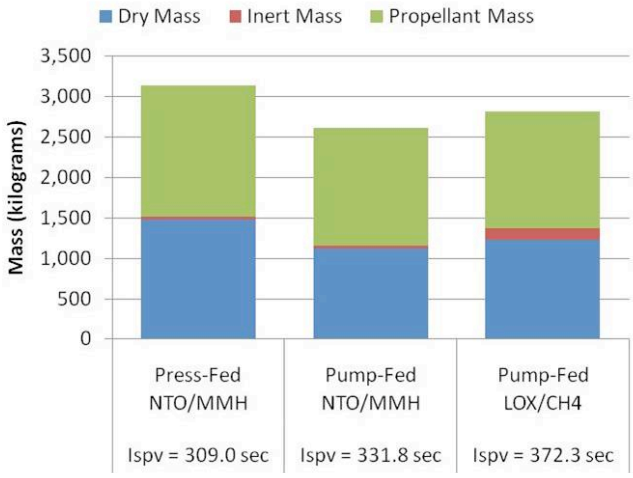

Figure 4. Propulsion Trade Results

This study, however, did not formally assess propulsion system risk. Future studies should carefully consider these issues.

Four pump-fed NTO/MMH engines for the main propulsion system (MPS) operate at 856 psia chamber pressure and a mixture ratio of 2.05 and are assumed to be derived from the RS-72 engine in development at Rocketdyne that delivers 12,000 pounds of thrust per engine [11]. Since stage thrust-to-weight (T/W) and engine area ratio were selected as independent variables, the required thrust varies from case to case and in the overall closure/optimization. Thus, a set of RSE's for the MPS were developed to quickly predict the engine characteristics as a function of required thrust and area ratio. The open circle in Figure 5 shows the engine T/W, specific impulse, engine length and engine exit diameter data used in the performance and sizing.

The MPS propellants are stored at 40 psia in two spherical graphite-wrapped aluminum tanks, one for NTO and one for MMH. Tank heaters and 10 layers of MLI provide thermal control for the tanks during the long interplanetary coast while a 6000 psia gaseous helium tank, constructed of graphite-wrapped aluminum, provides consumables for MPS tank pressurization.

The reaction control system (RCS) has sixteen pressure-fed thrusters each producing a thrust of 100 lbf. Each thruster operates at a chamber pressure of 125 psia, a mixture ratio of 1.65, and an area ratio of 40 delivering an Isp of 301.3 sec. The RCS propellants are stored at 225 psia in two spherical graphite-wrapped aluminum tanks, one for NTO and one for MMH. Tank heaters and 10 layers of MLI provide thermal control for the tanks during interplanetary coast while a 6000 psia gaseous helium tank, constructed of graphite-wrapped aluminum, provides consumables for RCS tank pressurization.

Ground rules of the study (Appendix A) required the total mass margin be 49.5% of the basic dry mass, which includes allocations for both mass growth allowance (MGA) and project managers reserve.

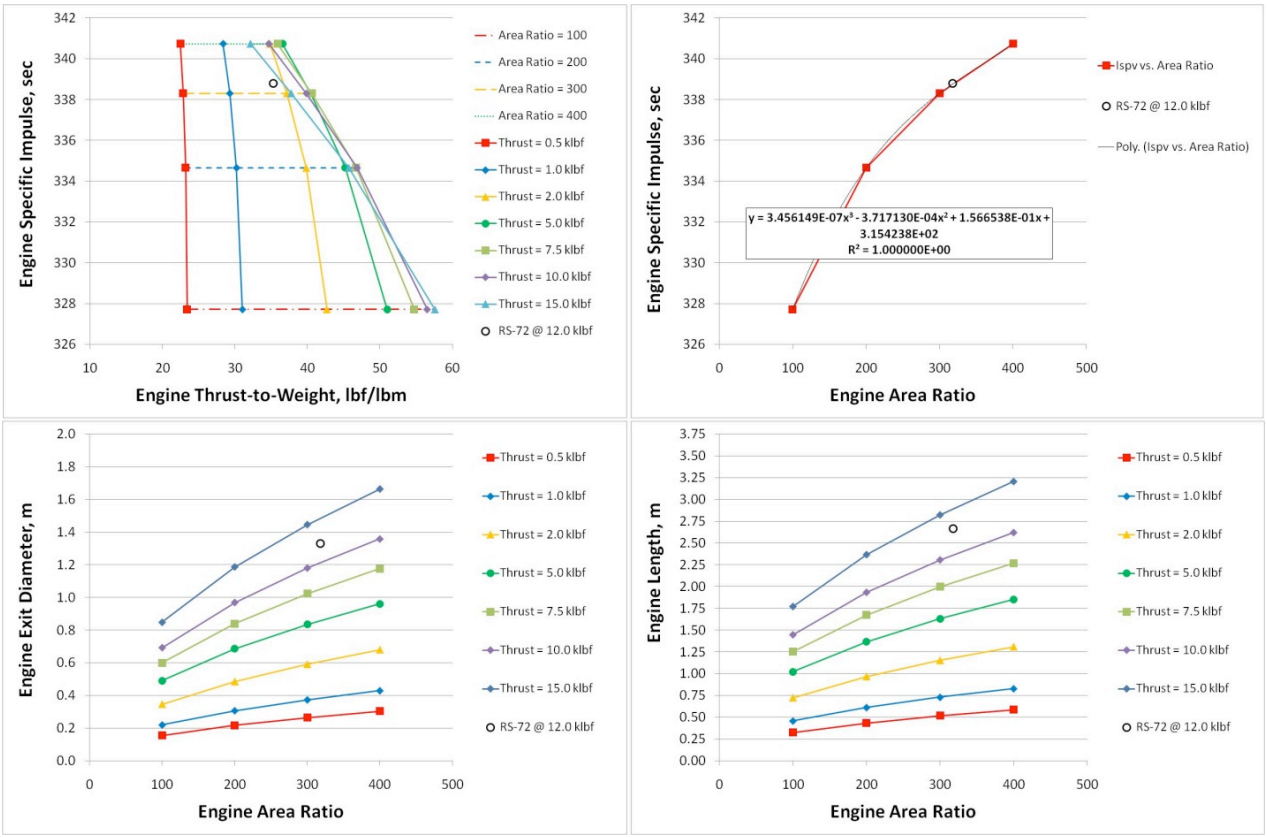

Figure 5. Parameteric Performance and Sizing Maps for a Pump-Fed NTO/MMH Rocket

A total of eight cases were evaluated: each of the four architecture concept cases was assessed using both an ablative and an insulating TPS.

Results for the eight cases assessed, summarized in Table 4, are EXAMINE verification results based on the final optimized solution provided by the POST2 analysis. The maximum payload delivered from a Delta IV-H, using the assumptions presented herein, occurs using the EFF-4 configuration, a direct entry at 5.8 km/s, which can deliver a payload of approximately 3.5 t.

Table 4. Mass Closure Results for each Architecture Concept

	EFF-1		EFF-2		EFF-3		EFF-4	
All Masses in kg	**Ablator**	**Insulator**	**Ablator**	**Insulator**	**Ablator**	**Insulator**	**Ablator**	**Insulator**
Descent Stage	**2,781**	**2,632**	**3,012**	**2,624**	**2,632**	**2,196**	**2,586**	**2,706**
Mars Aerocapture Stage	**1,809**	**2,206**	**1,304**	**1,988**	**1,271**	**1,727**	**1,170**	**906**
HIAD1 (Aerocapture)	974	1,429	0	0	0	0	0	0
Power System	221	221	221	221	221	221	221	221
HIAD2 (Entry)	614	555	1,083	1,767	1,050	1,506	948	684
Payload	**2,627**	**2,371**	**2,881**	**2,589**	**3,294**	**3,278**	**3,443**	**3,584**
Stack Mass at Launch	**7,217**	**7,209**	**7,198**	**7,201**	**7,197**	**7,200**	**7,198**	**7,196**

3.5 Recommendations for Future Enhancements

There are several areas that the EFF mass model can be improved in future studies:

HIAD

- Perform a trade study to better understand the relation between aeroshell stiffness and aerodynamic performance and its impact on aeroshell mass.
- Investigate whether aeroelastic behavior creates local high curvatures on the aeroshell producing localized high heating regions. This could have a significant mass penalty.
- Verify masses used for rigid load bearing components using a finite element analysis.
- Investigate the impact of maximum allowable fabric seam loads on inflatable mass.
- Design inflation system and determine the impact of leaks and ullage on mass.

Payload

- Determine the relation between minimum aeroshell diameter, angle attack, and payload height. The payload may be exposed to high thermal environment, and it may be required to be housed inside a shroud. The mass penalty for the shroud needs to be compared against flying at a lower angle of attack as well as smaller aeroshell diameter.
- Investigate whether a rover can be included with the payload.
- Investigate telescoping approach to shorten the payload height during EDL phase.

Overall

- Develop a higher fidelity model for packaging and assess associated mass penalties.
- Perform mass trade study for CG and bank maneuver mechanisms
- Develop viable separation concepts and determine the required mass penalty for each concept.
- Develop a better mass model for different guidance approaches.
- Investigate feasibility and risk of using pump-fed engines for exploration precursor missions.
- Perform a packaging effort to determine accurate inertias for 6DOF analysis.

4 HIAD Controllability Assessment

4.1 Overview

Five of the eight Year 1 Exploration-class architectures included large HIADs as the light-weight alternative to land large payloads. Controllability of HIADs is a major question regarding their feasibility, and thus a 6DOF simulation was developed in Year 2 with the intent of characterizing HIAD controllability. The Year 1 Exploration-class analysis assumed bank angle control similar to Apollo and MSL, which uses a bank acceleration of 5 deg/s^2 and a maximum rate of 20 deg/s. One objective of the EFF study (#5 in Sect 1) was to analyze alternative control strategies. Direct center of gravity (CG) control, which uses a mechanism to independently move the payload both vertically and laterally to generate lift and side forces, was selected for consideration. Additionally, the Year 1 study assumed a L/D of 0.25. Based on recommendations at the end of Year 1 to finding the lower L/D limit capability of HIADs, EFF considered vehicle L/D's down to 0.1. Because aerocapture is less complex than EDL, it was decided to use a 6DOF aerocapture mission for the controllability analysis. The trade study plan for assessing controllability included a L/D range of 0.1 to 0.25, atmospheric HIAD jettison and no jettison, and post-aerocapture target orbits of 500 km circular and 1 sol elliptical. In the absence of one guidance algorithm designed specifically for CG control, three available guidance algorithms and one new algorithm, developed and tested for bank control, were modified to accommodate CG control. What follows is a brief discussion of each guidance and control algorithm considered, as well as the description of the nominal aerocapture configuration and the results of the various trades performed to evaluate HIAD controllability.

Initial evaluation of the CG controller in the 3 DOF simulation looked promising. However, as the modeling fidelity was increased in the 6 DOF simulation, it became apparent that the CG controller, as assumed for EFF, did not have the control authority required to successfully fly the EFF architectures. Also initial analysis of actuator torques indicated that the power required to move the 2 to 4 t payload might be prohibitively high. The CG controller was replaced with the bank controller for all trade studies presented in this section. Acknowledging the incomplete CG controller assessment, EFF strongly recommends considering alternative CG controllers for HIADs in future system analysis studies.

4.2 Guidance Algorithms Considered

4.2.1 Hybrid Predictor-Corrector Aerocapture Scheme (HYPAS)

HYPAS is an analytical predictor-corrector algorithm that was developed and selected for the Aeroassist Fight Experiment, an aerocapture demonstrator mission that was canceled before launch. It has been used in numerous human and robotic exploration mission studies over the last 10 years for Earth and Mars, and has been proven to be robust to a wide variety of L/D, ballistic coefficients, atmospheres, entry conditions, and target orbits. It was considered for both the Mars Surveyor Program 2001 mission, and the CNES Mars 2005 Sample Return Orbiter, and later, the CNES Mars 2007 Premier Mission. Unfortunately all these missions were canceled before launch. HYPAS targets a lifting vehicle through the atmosphere to a desired exit orbit apoapsis and inclination by using an analytically-derived guidance algorithm based on deceleration due to drag and altitude rate error feedback to determine the bank angle magnitude, and the inclination error to determine bank direction.

4.2.2 Terminal Point Controller (TPC)

The TPC is an aerocapture guidance algorithm, closely related to the Apollo Earth Return entry guidance. TPC is based on the Calculus of Variations, with boundary conditions derived for the

aerocapture mission. Originally developed for the Mars Surveyor Program 2001 mission, it was later adopted by the French space agency (CNES) for the NASA-CNES Mars 2005 Sample Return orbiter. TPC is extremely robust and consists of a very little on-board code. A reference trajectory is defined for the aerocapture mission and that trajectory is used to develop sensitivities of the terminal point to changes in the lift vector at any point along the trajectory. These sensitivities are used to adjust the bank angle during flight to achieve the desired apoapsis at atmospheric exit. Lateral control is achieved by reversing the sign of the bank angle whenever the lateral error exceeds a variable-width deadband.

4.2.3 Numerical Predictor-Corrector Guidance (NPC)

The Numerical Predictor-Corrector algorithm was originally developed as candidate guidance for both the aerocapture and entry of the Mars Surveyor Program 2001 mission, and the aerocapture of CNES Mars 2005 Sample Return Orbiter. Orion developed NPC guidance for its lunar return. The NPC guidance integrates a simplified set of the equations of motion and iterates the appropriate control parameter to meet the specified constraints. For the EDL-SA architectures, the NPC guidance determines the bank angle profiles and the required propulsion orientation during terminal descent to provide the proper landing conditions. Because of the necessity to integrate the equations of motion, the NPC algorithm is only called every 10 sec as a worse case approximation. In reality the calculations take a fraction of that time.

4.2.4 Shape Integral (SI)

The Shape Integral aerocapture guidance is a new guidance algorithm developed at the Langley Research Center. This algorithm is based on an algebraic solution to the equations of motion in a plane. Normalized integral quantities, termed shape integrals, are calculated from a reference trajectory, providing the guidance gains. The velocity equation is first solved to determine the time-to-go. Then the altitude rate equation is solved for the appropriate scaling of a reference lift profile that is required to meet the targeted terminal conditions at atmospheric exit. Bank reversals are commanded to maintain a wedge angle, with respect to the target orbital plane, within set deadbands.

4.3 Control Algorithms

Two control actuation schemes were considered for the EFF vehicle. The first was bank angle control achieved by applying torques to the vehicle via an assumed RCS system. The second was vertical and horizontal lift control achieved by moving massive components, which shifted the center of gravity CG of the vehicle.

4.3.1 6DOF Bank Angle Controller

Bank angle control was performed using a Linear Quadratic Regulator (LQR) formulation. LQR provides a systematic approach to multi-input, multi-output control systems. The EFF controller is based on aircraft equations of motion that have been decoupled into longitudinal and lateral/directional subsets and linearized. Currently, it is assumed that pure torques about each vehicle axis are available at any level desired. The same controller structure is used for both the aerocapture and entry missions with different sets of gains.

4.3.2 6DOF Center of Gravity (CG) Controller

The CG controller is actually a combination of CG control and a small RCS system to provide roll control. A single PID controller commanding a pure roll torque to drive the roll angle to zero provides roll control. In the vertical and horizontal channels, the guidance provides a commanded lift. Each of those commands is passed to a PID controller, which commands a payload position. The payload position

command is passed to a second order actuator model, which moves the payload and the resultant CG is computed by the POST2 trajectory simulation. Forces to move the payload are assumed to be as large as necessary, but the actuator limits payload rates and accelerations.

4.4 Exploration Feed Forward Nominal Configuration

4.4.1 Nominal Configuration Inputs

The primary nominal aerocapture parameters used in the controllability analysis are given in Table 5. Additional parameters are provided in Appendix D.

Table 5. Nominal Aerocapture Parameters

Parameter	Value
Aeroshell Diameter	14 m
Vehicle Diameter	4 m
Ballistic Coefficient	33 kg/m^2
Lift-to-Drag Ratio	0.25
Target Orbit	500 km circular
Entry Flight Path Angle	Guidance dependent

These inputs are used to create the baseline EFF aerocapture configuration. The HIAD diameter was sized to satisfy a 3-sigma peak heat rate constraint of 50 W/cm^2 keeping in mind the minimum diameter constraint to prevent flow impingement. Also the budgeted delta-V required to clean up the post-aerocapture orbit to match target orbit was constrained to 250 m/s. The clean up burn was modeled as a 3-burn maneuver that included (1) an apoapsis raise/lower maneuver, (2) a plane change maneuver and (3) a periapsis raise maneuver.

The Monte Carlo dispersions used in this analysis are given in full detail in slides 5 through 7 of Section 7.2 of the slide package presented at the IPR [12]. These dispersions were chosen to be intentionally overly conservative in order to stress the guidance. 8000 cases were run for each set of Monte Carlo results.

4.4.2 Aerocapture Monte Carlo Results

Figure 6 shows aerocapture heat rate and ΔV results for an L/D of 0.25 into a 500 km circular orbit. The histogram of heat rate shows these cases essentially met the 3-sigma peak heat rate requirement by not significantly exceeding 50 W/cm2, and the maximum delta-V required to cleanup the post-aerocapure orbit never approaches the 250 m/s budget. Additionally, the apoapsis values in this configuration form a very tight group around 500km, which demonstrates that an L/D of 0.25 is sufficient to hit the target apoapsis for this entry speed and target orbit.

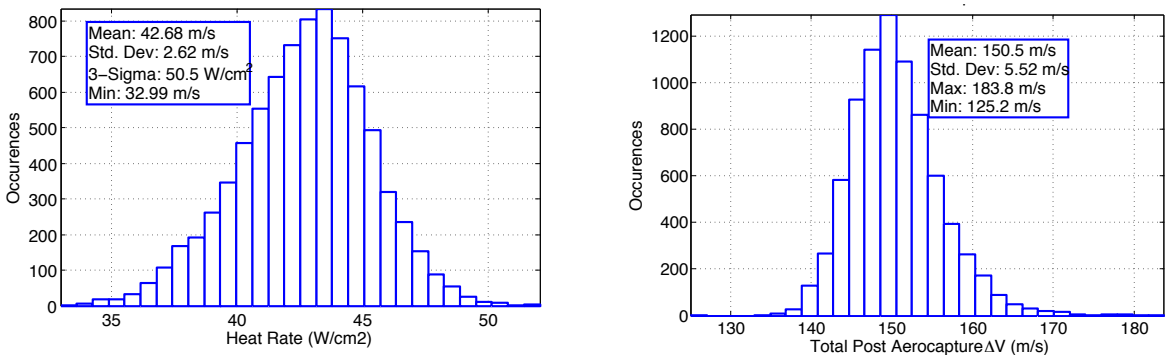

Figure 6. Heat Rate and Total ΔV for EFF-1 Aerocapture

4.4.3 Trade 1: L/D of 0.1 Versus L/D of 0.25

Figure 6 shows that an L/D of 0.25 is sufficient to hit the target orbit apoapsis with the inputs and Monte Carlo dispersions listed in Table 5 and the references. Based on inquiries from both Year 1 and other technology programs (i.e. IRVE), a trade was performed to determine if the vehicle would still meet the target apoapsis, given less commandable lift. Therefore, this study considers differences in performance associated with flying at an L/D of 0.25 and an L/D of 0.10.

Figure 7 shows the Monte Carlo results of the apoapsis and periapsis altitudes for a L/D of 0.10 and 0.25. The vehicle with the L/D of 0.10 is still able to reach the target apoapsis, but inspection of the performance associated with individual lower L/D cases shows instances where the guidance is fully saturated. Guidance saturation occurs when the guidance must command maximum lift for the entire trajectory, leaving it no authority to fly out additional dispersions. To remedy this, the lateral corridor width is expanded for the lower L/D cases resulting in larger plane change maneuver delta-V, as shown in Figure 8.

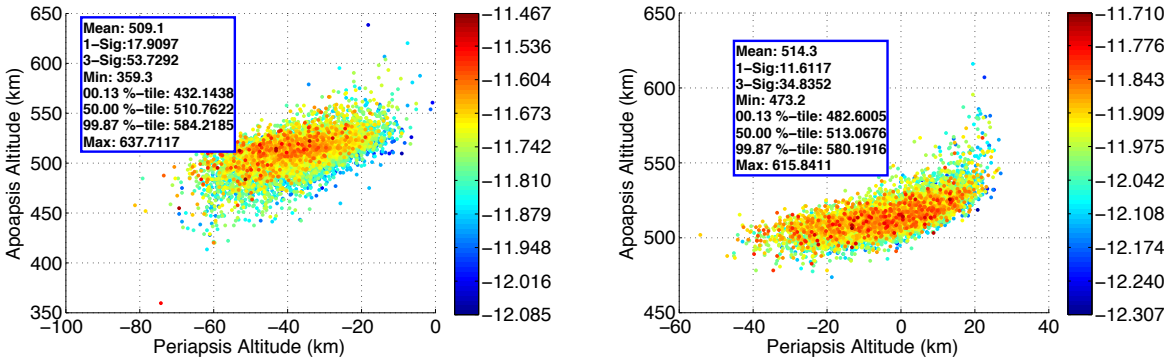

Figure 7. Apoapsis Altitude vs Periapsis Altitude for L/D = 0.10 (left) and 0.25 (right)

This study shows that aerocapture using a low L/D vehicle is feasible but will likely result in larger propellant use. Additionally, these results are specific to the EFF configuration described. Changes to target orbit or entry speed may result in cases that are unable to reach the target apoapsis for a lower L/D vehicle.

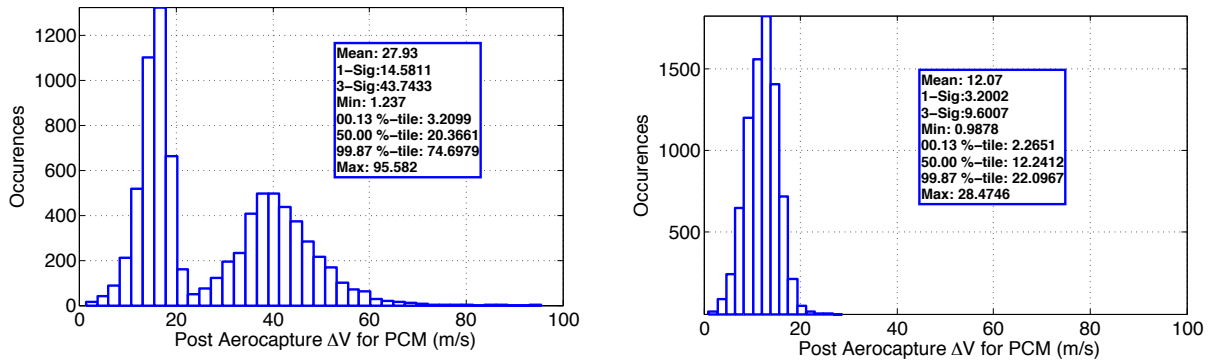

Figure 8. Plane Change Maneuver ΔV for L/D of 0.10 (left) and 0.25 (right)

4.4.4 Trade 2: Jettison Versus No Jettison

Analyzing the results from the L/D trade study, specifically those from guidances that were unable to reach the target apoapsis for the lower L/D vehicle, led the team to consider alternatives that might improve low L/D performance. Realizing that better performance might be achieved by adding an additional control parameter, consideration was given to analyzing the effect of jettisoning the HIAD atmospherically. This prompted the following trade study.

In an attempt to increase the ability of a specific guidance to hit the target orbit apoapsis, a subroutine was placed in the guidance, which used the current navigation states to calculated apoapsis at each time step. Once that calculated apoapsis reached a specified value, the HIAD would be released and the vehicle would go from a lifting body to drag only. The jettison was modeled as a step function in the simulation, where at one time step the HIAD is attached and the next it is released. Jettisoning the HIAD in the atmosphere also allows aerodynamic forces to aid in separation. However, details of HIAD separation were not considered in this study.

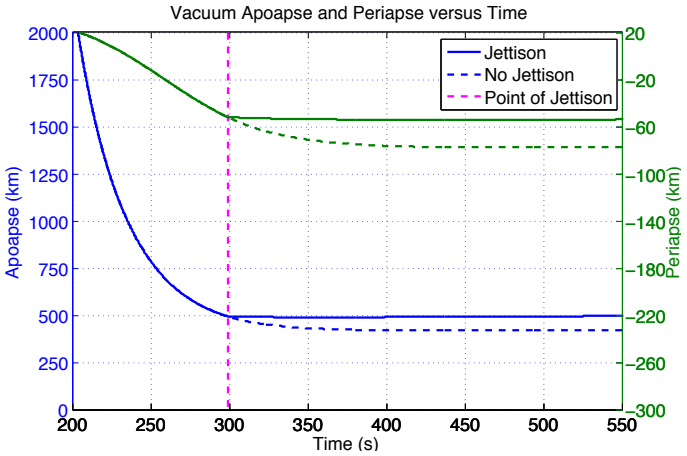

Figure 9. Vacuum Apoapsis and Periapsis Altitude vs. Time With and Without HIAD Jettison

The disadvantage of jettisoning the HIAD in the atmosphere is that it only aids in hitting the apoapsis target when the guidance targets an apoapsis value below the desired target. This requires a much steeper flight path angle and can result in guidance saturation as well as higher heat rates. The advantage of jettisoning the HIAD is that it allows the vehicle to hit very close to the target apoapsis every time by essentially fixing the apoapsis value at the jettison point and allowing the vehicle to coast to a lower value, as illustrated in Figure 9.

This trade study considers the effect of the jettison vs. no jettison for vehicles with an L/D of both 0.10 and 0.25. The first part of this study was performed for an L/D of 0.10, to determine what benefit the jettison maneuver might provide. Figure 10 shows the difference in apoapsis and periapsis values between the jettison and no jettison cases. By essentially fixing the apoapsis and periapsis values at the jettison point, the jettison maneuver allows the vehicle to hit the target with much better accuracy than the no

jettison case. The smaller distribution in apoapsis and periapsis altitude values is reflected in Figure 10. The reduction can also be seen in distribution of periapsis raise maneuver ΔV shown in Figure 11. The four points in left of Figure 10 that are above 550 km are the cases where the calculated apoapsis value never reached the HIAD jettison condition, thus the HIAD remains attached for the duration of the flight.

The second part of the study was performed for an L/D of 0.25 to determine if the benefits of the jettison maneuver persist at higher values of L/D. The observed effect of the jettison maneuver was a tightening of both the apoapsis and periapsis performance. This is evident in Figure 12. However, the performance associated with the higher L/D no jettison cases suggest that no additional control parameter is necessary to help these cases reach their target orbit apoapsis.

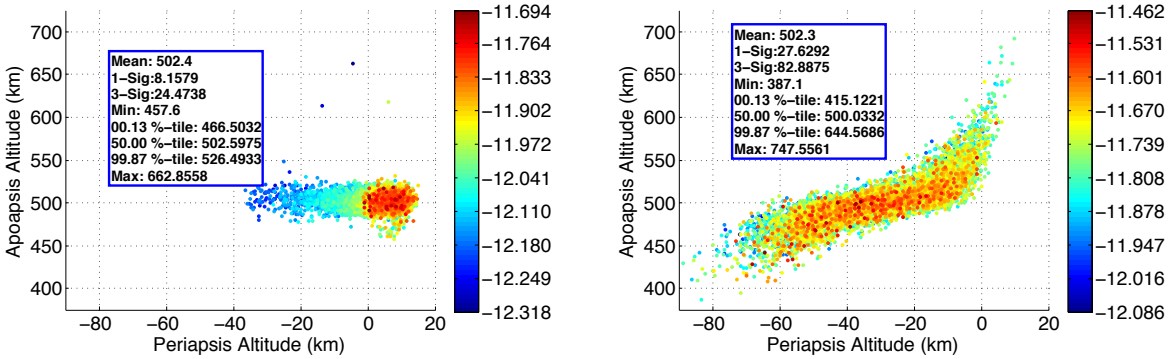

Figure 10. L/D = 0.10: Apoapsis vs. Periapsis Altitude for Jettison (left) and No Jettion (right)

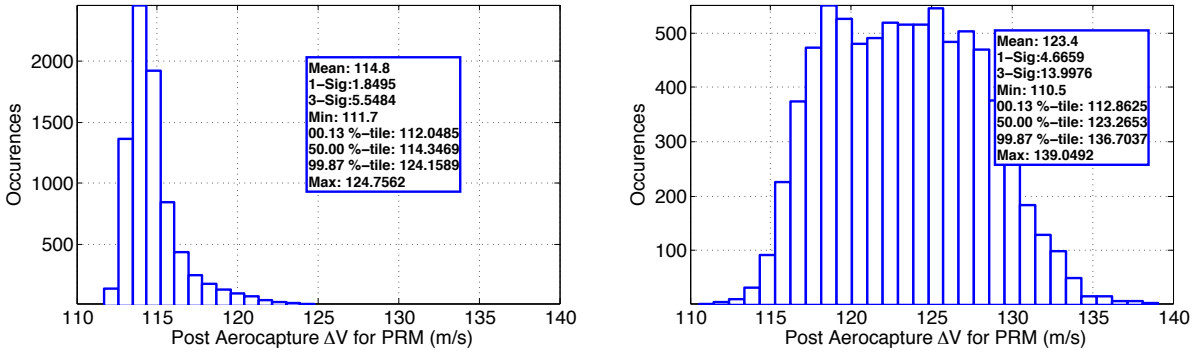

Figure 11. L/D = 0.10: Periapsis Raise Maneuver DV for Jettison (a) and No Jettison (b)

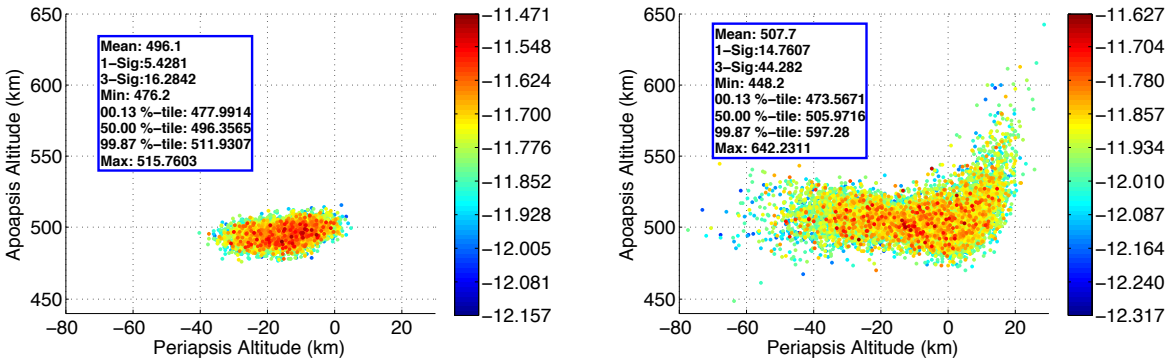

Figure 12. L/D = 0.25: Apoapsis vs Periapsis Altitude for Jettison (a) and No Jettison (b)

In summary the jettison maneuver does improve the vehicle's ability to achieve a target orbit for any L/D. The necessity for the jettison maneuver becomes less critical at higher values of L/D and the decision to employ jettison for higher L/D vehicles will depend on mission specific requirements. Additionally, the modeling of the jettison maneuver is crude and factors such as HIAD separation and transitions would need to be considered if this concept were to be studied further.

4.4.5 Trade 3: L/D of 0.25 with 500 km Circular Target Orbit Versus 1 sol Target Orbit

One final trade study was performed to determine the effect of changing the post-aerocapture target orbit for a vehicle with an L/D of 0.25. The apoapsis altitude associated with a 1 sol target orbit is 33,793 km, making it a much higher target apoapsis, requiring less energy (or ΔV) change compared to the 500 km circular orbit. The aerocapture maneuver performance is improved when more energy can be removed from the aeropass, therefore targeting a much higher apoapsis makes executing the aerocapture maneuver more difficult. For the higher apoapsis orbits, velocity error is associated with a large error in target apoapsis altitude, which will require a larger ΔV to correct. Additionally, the lack of available corridor coupled with velocities that approach exit speeds creates the possibility of some single pass cases that do not capture into orbit.

Figure 13 shows a comparison of apoapsis and periapsis altitudes for the two target orbit cases. Noting the difference in plotted scales, the 500 km circular orbit has a much smaller distribution. However, the 1 sol cases spend less time in the atmosphere and are able to maintain much higher periapsis values. The benefit is evident in the ΔV required to clean up the periapsis altitude error. The 500 km circular orbit requires almost ten times as much ΔV (average 125 m/s) than the 1 sol orbit (average 13 m/s). When the apoapsis clean up burn is included, the *total* (periapsis + apoapsis + wedge angle burns) ΔV required for the different orbits is, on average 150 m/s for the 500 km circular orbit and 40 m/s for the 1 sol orbit.

In comparing the two target orbits, it is evident a large ΔV savings is achieved by changing to a target orbit with a higher apoapsis altitude but the propellant savings is at the cost of increased risk of skip-out. The results of this trade study are specific to the mission assumptions outlined here. Further work is needed to completely characterize the risk of skipping out of high-energy orbit as the L/D or approach velocity decreases.

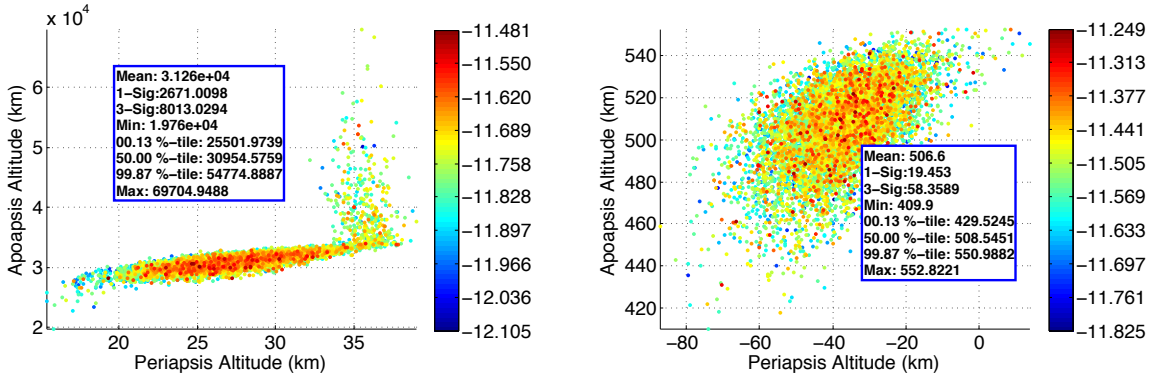

Figure 13. Apoapsis vs. Periapsis Altitude for the 1 sol (left) and 500 km circular (right) target orbits

4.5 HIAD Controllability Conclusions

Despite the results shown in the previous section, the HIAD controllability study is incomplete due to the lack of a full assessment of the CG controller. However, the information learned by evaluating guidances using the bank angle controller did reveal useful information for current and future studies.

First, the nominal EFF aerocapture mission using a L/D of 0.25 provides sufficient targeting capability while satisfying the constraints. Second, during the EFF study, the IRVE 4 team has uncovered potential dynamics due to flexure at the joint between the rigid heat shield and the HIAD that need to be included in future systems analysis studies. Third, the bank angle control was marginal (large number of trajectories saturated) for an L/D = 0.10 with no HIAD jettison. Forth, jettisoning the HIAD while in the sensible atmosphere indicates a capability to improve targeting, but more analysis is required to determine if it is a viable option. Finally, CG control was demonstrated in 3DOF trajectories to be a viable option, however, the 6DOF analysis uncovered issues that require further examination. The primary issue concerns how using CG control to both control and trim the vehicle induces dynamics that may require large actuator accelerations. One recommendation is to add other CG control options to the design space, which, for example, uses the CG control for trim and an RCS system to control the induced dynamics.

5 ALHAT Sensor Assessment

The objective of the ALHAT sensor assessment for EFF was to develop a 6DOF entry simulation to determine the sensor performance ranges for an ALHAT-like navigation and sensor system at Mars. The EFF simulation was developed and used to run initial integrated GNC and sensor performance and evaluate of SRP for Hazard Detection and Avoidance (HDA) and Terrain Relative Navigation (TRN). The EFF simulation included 6DOF entry with Apollo entry guidance and an LQR bank angle controller and 3DOF powered descent with Apollo powered descent guidance and a pseudo controller. The ALHAT Extended Kalman filter (EKF) is also included in the simulation, but it did not include TRN update capability. However, statistically-based IMU, startracker, altimeter and velocimeter models were integrated in the simulation and utilized in the analysis.

The Apollo entry guidance, showing integrated guidance and controller performance with 6DOF entry Monte Carlo results are shown in Section 6.1. The SRP powered descent study and trajectory design and sensor feasibility is presented in Section 6.2 with 3DOF descent Monte Carlo results and flight condition assessments for HDA and TRN at Mars. Section 6.3 discusses initial results of the fully integrated GNC system & sensor performance, focusing on the ALHAT navigation filter, with 6DOF entry and 3DOF descent Monte Carlo results, without TRN versus an ideal TRN case for comparison.

5.1 Entry Guidance Performance

The entry guidance used in the Study is an Apollo-derived entry guidance. The Apollo-derived entry guidance algorithm is a terminal point controller that steers the vehicle to a HIAD separation point though bank commands that are based on deviations in range, drag acceleration and altitude rate from a stored reference trajectory (Figure 14). In the reference trajectory, the bank value of 45° for the constant bank phase is based on the expression

$$\text{Bank}_{\text{min}} = \text{acos}(100\%-\rho\%-C_d\%),$$

where $\rho\%$ and $C_d\%$ are the dispersions in atmospheric density and on the drag coefficient, respectively. The lateral corridor is determined such that the number of reversals is 3 (the bank reversal deadband quadratic coefficients are 0.025 [first reversal] and 0.064, with the deadband constant coefficient being 0.5). The nominal final altitude of the reference trajectory is determined such that all the powered descent dispersed cases are successful.

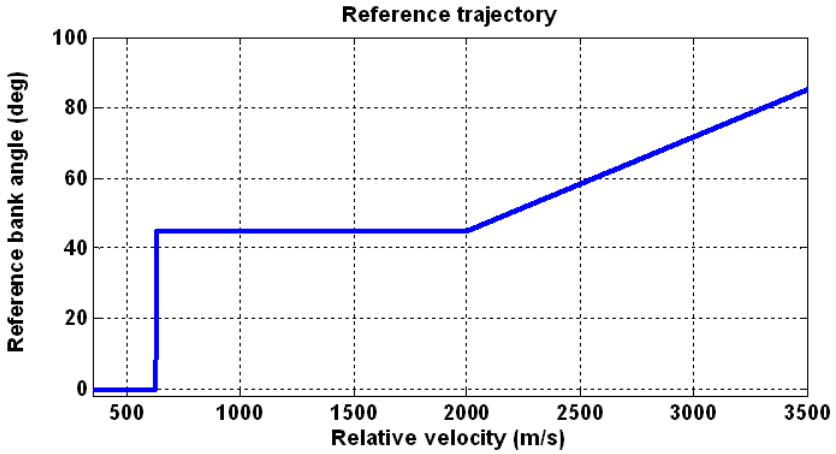

Figure 14. Reference Bank Profile

The performance was assessed using 6DOF Monte Carlo analysis comprised of 8000 runs with simple propagator navigation (Figure 15). The L/D overcontrol gain used is 2 and the overcontrol gain of

the heading alignment phase is 60. Downrange error is not shown because the simulation end condition is based on range, thus, the downrange error is very small at separation. Downrange error at engine initiation is within ±200 m. The dispersions used in this phase are found on Appendix C.

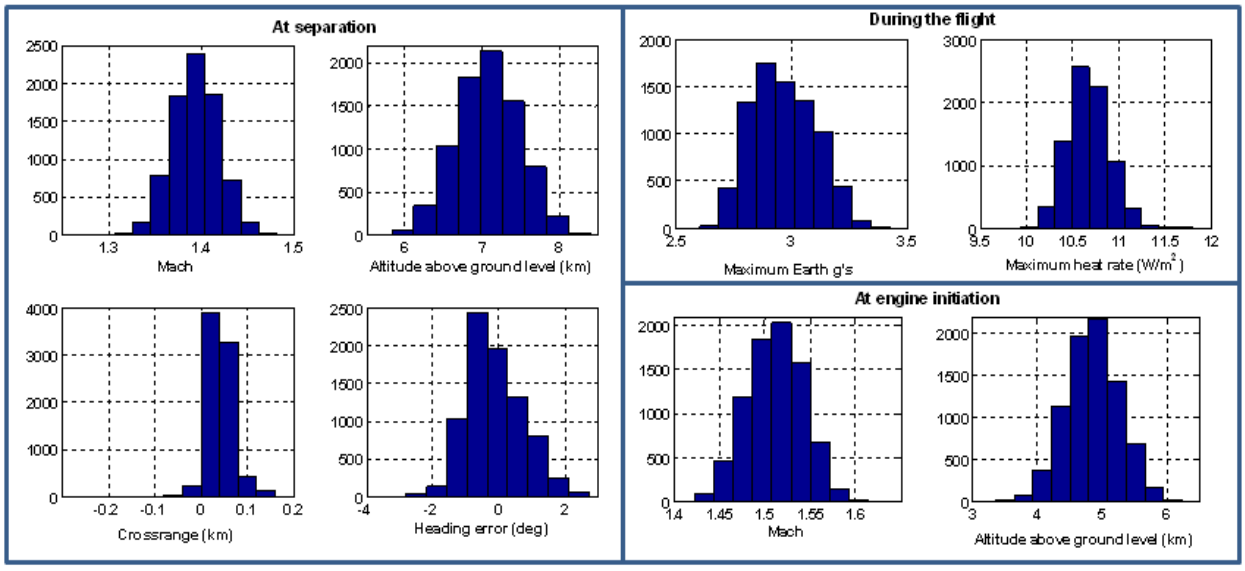

Figure 15. Entry Performance Summary

Using the defined dispersions, the design of the entry guidance is capable of achieving the engine initiation conditions such that all the powered descent dispersed cases can be landed successfully. However, this design of the entry guidance should not be considered as a final design. There is room for improvement by fine tuning and improving the guidance parameters that affect the performance (reference profile, over-control settings, initial flight path angle, drag acceleration and L/D filter time constants and the drag and altitude controller gain scale factors).

5.2 Powered Descent Performance

The objective of the powered descent is to steer the vehicle to a controlled touchdown using the main propulsion engines. The following assumptions were made for the powered descent analysis:

- Apollo LM-derived guidance (2nd order polynomial in acceleration)
- Initial states for powered descent from entry Monte Carlo results
- 3-DOF pseudo control with 20 deg/sec and 5 deg/sec^2 attitude limits
- Perfect navigation
- Target touchdown velocity is 1 m/s vertical, 0 m/s horizontal
- Fly out all position error prior to touchdown
- 8000 case Monte Carlo
- Dispersions as shown in Appendix D

The termination conditions for entry were chosen such that all dispersions could be removed with the minimum amount of fuel. If the termination altitude for entry were lower, some cases would not be able to successfully achieve the target touchdown conditions. If entry were to end at higher altitude, additional fuel would be needed for powered descent. The 99.87%-tile value for propellant consumed was 870.5 kg.

The 0.13%-tile value for propellant remaining at touchdown was 249.5 kg. Given the current dispersions and entry performance, the powered descent has sufficient propellant margin. Further study showing the effect of navigation on powered descent was completed and is discussed in Section 5.3.

5.2.1 TRN and HAD Feasibility

A brief investigation of feasibility of both TRN and HDA was undertaken. TRN works over a wide range of altitude and velocity and is possible anytime sensor measurements can be taken and a high-quality map of the terrain is available. There are two basic forms of TRN; optical TRN, which uses optical cameras in the visible spectrum, and active TRN, which uses an altimeter, flash lidar, or other active sensor. Fundamentally, all that is needed is to ensure that this sensor has a view of the surface and that the navigation has a reasonable estimate of the vehicle's inertial position. Since the attitude profile during the first 60 sec is well off of the vertical (see Figure 16), it can reasonably be assumed that TRN measurements can be taken and that TRN is feasible.

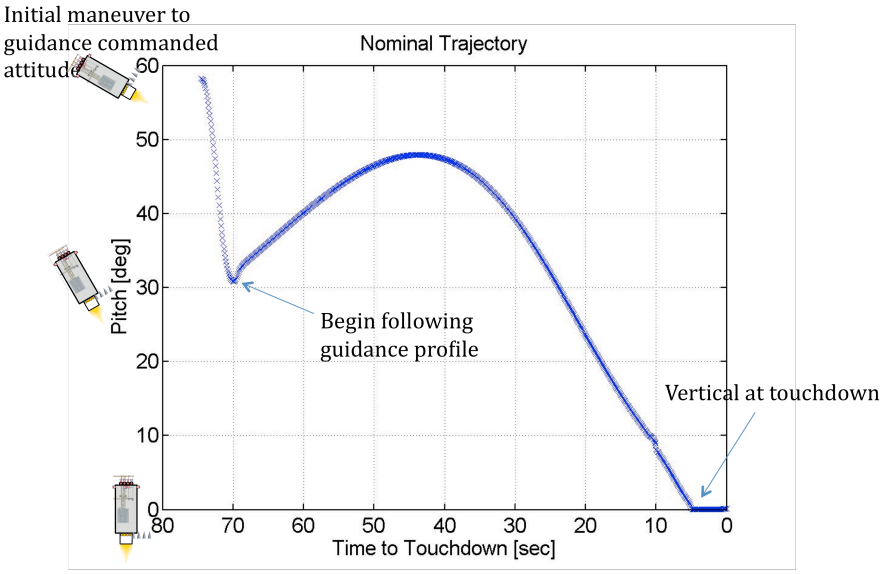

Figure 16. Pitch Profile During Powered Descent

Feasibility for HDA is more complex to demonstrate than for TRN. The flash lidar must scan the landing area, so it requires a line of sight to the landing area at the correct time during the descent. The lidar will be designed for optimum performance at a particular slant range from the landing site. The scan must occur at this distance to ensure that sufficient resolution is achieved and the full landing area can be scanned.

An initial analysis of the nominal trajectory shows that HDA is feasible for the nominal by looking out the back side of the vehicle (in the same direction in which TRN would occur) at an altitude of 1 km. However, in dispersed cases the look angle may be close to zero and the distribution may be both positive and negative at the time of the scan. This would require two sensors, one on each side of the vehicle. The trajectory can likely be redesigned such that all look angles are positive, for a minimal cost in additional propellant usage – and only would require one HDA sensor. Further investigation is needed before a conclusive determination can be made regarding HDA feasibility.

5.3 Navigation Performance

The ALHAT navigation filter used in the study is an EKF that provides estimates of the vehicle state (inertial position, inertial velocity and attitude quaternion). The EKF uses the IMU for propagation while it receives updates (in the form of altimeter, startracker, velocimeter and TRN measurements) to improve state estimation. The ALHAT EKF initial performance and functionality was analyzed by running two Monte Carlo simulations, one with and one without TRN measurements. Since the delivery of the filter did not contain a TRN update capability, TRN measurements were mimicked using the simple propagator navigation filter for a comparison case. The following assumptions were used in the ALHAT EKF Monte Carlo:

- 2000-dispersed cases
- Same aerodynamic, atmosphere and initial state dispersed inputs as aerocapture Monte Carlos (Appendix D)
- Dispersed sensor inputs (Appendix E)
- 6DOF entry with Apollo entry guidance and LQR controller
- 3DOF powered descent guidance and pseudo controller
- Startracker measurements off at entry interface
- Altimeter measurements start at engine ignition
- Velocimeter measurements start at 2 km altitude
- No TRN

The comparison Monte Carlo has the same assumptions as the ALHAT EKF Monte Carlo, but was run with simple propagator navigation filter reducing navigation error manually during SRP to mimic TRN updates of an ideal ALHAT system. Three 'mock' TRN measurements were taken at 5 km, 2 km and 1 km altitudes.

Inertial navigation position and velocity error throughout the trajectory, as well as range-to-target at touchdown, were parameters used to initially evaluate the ALHAT EKF performance. At deorbit, or simulation initialization, initial inertial position navigation error was 3.5 km (99.87%-tile) and inertial velocity navigation error was 3.5 m/s (99.87%-tile). These errors are very conservative and may be adjusted with sensor measurement updates prior to deorbit. The resulting inertial navigation position error at entry was improved through propagation of the IMU updates to 3 km (99.87%-tile) and inertial velocity error was 3 m/s (99.87%-tile). The altimeter updates in the ALHAT EKF Monte Carlo began at engine ignition (nominally, 6 km altitude) and improve the altitude navigation error from 3.4 km (44% error) down to 11 m (1% error) (99.87%-tile), also improving inertial navigation position error from 4 km down to 2.8 km (99.87%-tile) at touchdown. The velocimeter updates in the ALHAT EKF Monte Carlo began at a 2 km altitude and improve relative velocity error from 3 m/s (1% error) down to 2 cm/s (0.01% error) (99.87%-tile), also improving inertial navigation velocity error from 5 m/s down to 17 cm/s (3-sigma). Fuel remaining at touchdown was similar to powered descent study results with perfect navigation discussed in Section 6.3. The results showed good initial ALHAT EKF performance. The range-to-target at touchdown, using the navigation updates and SRP, can get within 2.4 km (99.87%-tile) of the landing target. However, more improvement in navigation position error is needed to reduce the touchdown footprint.

The ALHAT EKF Monte Carlo (no TRN) was compared to an ideal TRN Monte Carlo where three TRN updates were mimicked as position navigation error reductions down to 85 m (conservative, based on ALHAT project analysis) during SRP. Results showed that inertial navigation position error was

reduced from 4 km at engine ignition down to 125 m (99.87%-tile) at touchdown, compared to a reduction down to only 2.8 km (99.87%-tile) from the ALHAT Monte Carlo results. Improvement in navigation position error in form of TRN updates is needed to reduce the touchdown footprint.

Figure 17 shows scatter plots of downrange and crossrange for both Monte Carlos at engine ignition and touchdown. TRN updates are needed to get within 100 m (99.87%-tile) of the landing target.

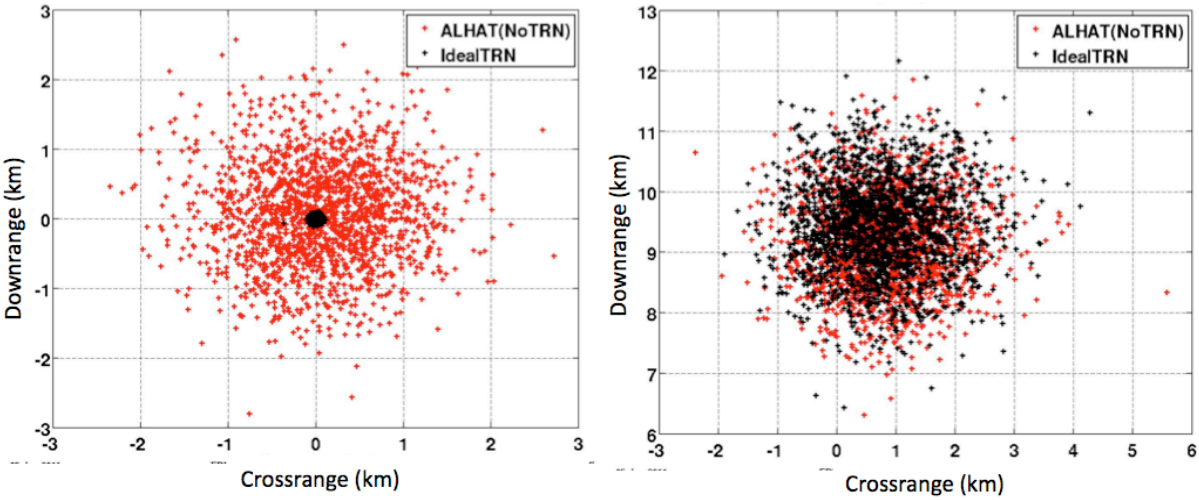

Figure 17. Range Scatter Plot Comparison at Engine Ignition and Touchdown.

The initial results of the ALHAT EKF performance analysis show good navigation performance using SRP (with altimetry and velocimetry updates) and initial TRN comparison during descent to reduce navigation position error for precision landing. SRP during descent and altimetry and velocimetry navigation updates can get within 2.4 km of the landing target (99.87%-tile). However, TRN (or similar sensor) is needed to get landing accuracy down to 100 m (99.87%-tile) or less. For future work, TRN update capability in ALHAT EKF is needed to fully assess ALHAT navigation performance and to study TRN operating ranges and timing trades.

5.4 Recommendations and Future Work

As a result of the study, the following investments are recommended:

- Examine ALHAT-developed sensors for use in Mars EDL (to include laser altimeter, Doppler lidar velocimeter, and flash lidar)
- Perform additional performance and feasibility studies concerning the use of TRN for Mars EDL
- Investigate adapting HDA for Mars EDL and the effect on vehicle design

Future Mars EDL studies should consider performing the following work:

- Update current baseline navigation and integrated GNC performance with latest filter and sensor models
- Update ALHAT sensor models and operating ranges for Mars
- Update Star tracker operating range and conditions
- Perform GNC performance sensitivity to measurement quality and availability
- Perform early TRN Study

- Trade timing, number of TRN measurements. Consider feasibility of performing TRN prior to Powered Descent.
- Perform divert sensitivity study
- Perform detailed HDA analysis for Mars landing
- Consider terrain, landing footprint size including GNC errors, lidar performance, etc.

6 Conclusions

This document attempts to summarize the analysis performed to evaluate feed forward technologies in a realistic but hypothetical mission to land a 2 to 4 t power plant on Mars. Table 1 in Section 1 presents the major technology recommendations that resulted from the analysis presented in Sect 4, 5 and 6. Much of the EFF effort focused on detailed subsystem model development, which uncovered many unanticipated issues. The remaining time was spent upgrading the POST2 simulation to incorporate and check the detailed models. Consequently, the analysis results were incomplete in some aspects as the team prepared of the final EDL-SA technical meeting, the EFF IPR. Software configuration management proved to be instrumental in allowing for rapid analysis of all aspects of the design late in the project schedule. The major recommendation from EDL-SA is that high fidelity systems analysis can leverage work being done at many NASA centers to identify advantages and disadvantages of specific technologies considered for investment.

7 Bibliography

1. Dwyer Cianciolo, A. M., et al. " Entry, Descent and Landing Systems Analysis Study: Phase 1 Report." NASA/TM-2010-216720
2. Drake, B. G., editor., "Human Exploration of Mars Design Reference Architecture 5.0," s.l. : NASA-SP-2009-566, July 2009
3. Entry, Descent and Landing Systems Analysis (EDL-SA) for High Mass Exploration and Science Mars Mission Systems: Final Report, EDLSA-005, January 2011 (unpublished)
4. Mason, L. S., "A Summary of NASA Architecture Studies Utilizing Fission Surface Power Technology," AIAA-2010-6599.
5. Samareh, J. A., and Komar, D. R., "Parametric Mass Modeling for Mars Entry, Descent and Landing System Analysis Study," AIAA-2011-1038, presented at the 49th AIAA Aerospace Sciences Meeting including the New Horizons Forum and Aerospace Exposition, Orlando, Florida, Jan. 4-7, 2011
6. McGuire, M.K., Arnold, J. O., Covington, M.A. and Dupzyk, I. C. "Flexible Ablative Thermal Protection Sizing on Inflatable Decelerator Systems Technology for Human Mars Entry, Descent and Landing, AIAA Conference, Orlando FL, January 2011 AIAA-2011-344
7. Beck, R. A. et al. "Overview of Initial Development of Flexible Ablators for Hypersonic Inflatable Aerodynamic Decelerators", 21st AIAA Decelerator Conference and Seminar, 23-26 May2011,Trinity College, Dublin, Ireland
8. Komar, D.R., Hoffman, J., and Olds, A., "Framework for the Parametric System Modeling of Space Exploration Architectures," AIAA-2008-7845, 2008
9. http://www.astronautix.com/props/hydazine.htm
10. http://en.wikipedia.org/wiki/Atlas_V
11. http://www.spaceandtech.com/spacedata/engines/rs72_specs.shtml
12. Dwyer Cianciolo, A. M., et al. "Entry, Descent and Landing Systems Analysis Exploration Feed Forward Internal Peer Review Slide Package". NASA/TM-2011-217050

8 Appendix A - Design Reference Mission, Ground Rules and Assumptions and Evaluation Criteria

This material is taken directly from Entry Descent Landing Systems Analysis for Large Robotic and Human Precursor Class Missions. Report of the Design Reference Missions, Ground Rules and Assumptions and Evaluation Criteria, EDLSA-004, June 28, 2010, and is included here for convenience.

8.1 Design Reference Mission

A Design Reference Mission (DRM) describes the objectives and top-level requirements for a representative future mission for the purposes of facilitating choices of architectures and technologies for a class of missions. The EDL-SA Year 2 Study encompasses two such classes—MSL-Improvement and Feed Forward. This section provides a summary of the respective DRMs for these two mission classes that will be used in the EDL-SA Study.

This section provides a summary of the respective DRM that will be used in the EDL-SA Feed Forward Study.

The DRM for the Feed Forward Study mission is designed to address technical issues identified in EDL-SA Year 1 that affect development planning. The configuration is based on results from Year 1 work, which indicated that the masses of a single use HIAD for aerocapture and a single use HIAD for entry might offer a lighter arrival mass option compared to a single dual use ablator TPS HIAD (Year 1 Architecture 2 and 6) provided heat rates could be kept below 50 W/cm2. Since the Feed Forward study considers the precursor mission class, the payload mass is much smaller (~2 t) compared to the Year 1 study (40 t payload).

Therefore, the DRM for the Feed Forward effort includes an insulator TPS HIAD for aerocapture into a 500 km circular orbit. After some TBD time the HIAD is jettison prior to entry. Also in orbit prior to entry, the second HIAD is inflated. A deorbit burn is initiated and the vehicle enters the atmosphere of Mars at ~3.35 km/s. From the results of the Year 1 study, it was not clear whether bank angle control is feasible especially for HIADs with very large diameters. The decision was made to consider alternative modes of HIAD control. For this reason, center of gravity control has been considered for the nominal control method for the Feed Forward architecture. A full evaluation will be made regarding the control authority required and by the vehicle compared to the control authority physically available within the packaged vehicle. The vehicle will use a theoretical guidance to fly to a specified target. At Mach = ~2, the supersonic retro-propulsion will be activated and used to complete the terminal descent. Finally, the vehicle will slow to 1 m/s and maintain that velocity for five seconds prior to touch down at 0 km above the MOLA areoid. An illustration of the nominal DRM is provided in Figure 18. Table 6 provides a list of key parameters for the Feed Forward DRM. The notional payload for this DRM is a Movable Nuclear Power System (MNPS) [4], described in "A Summary of NASA Architecture Studies Utilizing Fission Surface Power Technology" and illustrated in Figure 2. For this uncrewed DRM, the H_2O Shield is unnecessary. The CBE mass of the remaining components of the MNPS is approximately 2 t for the 10 kWe system. To this payload must be added the mechanisms necessary to deploy the payload on the surface and the margins. This DRM is in conjunction with an additional lander with the demo system to be powered by the MNPS, e.g., an ISRU demo. The Feed Forward Study only considers the single mission for deploying the MNPS, using this payload (for which a detailed MEL and a CAD model exist) for representative volume, mass and inertias of a Feed Forward mission payload.

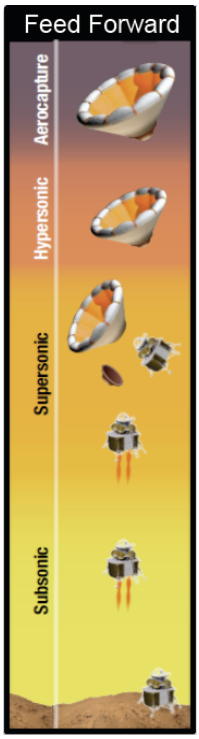

Figure 18. Feed Forward DRM

Table 6. Key Parameters for Feed Forward DRM

Parameter	Value
Launch	
Vehicle	Delta IV-H
Shroud Diameter	5 m
Launch C3	15 km2/s2
Arrival	
Velocity	7.3 km/s
Mass	7.2 t
Orbit	Aerocapture into a 500 km circular orbit
HIAD Shape	65 deg sphere cone
Entry	
Velocity	3.35 km/s
HIAD Diameter	TBD
Nominal Control Method	Center of Gravity
SRP Mach range	Mach >2
Payload	>=2 t
Mass Properties	TBD
Loads paths and Attach points	TBD
Date	
Landing Altitude	0 km MOLA
Landing Precision	<50 m
Keep Out Zone	1 km

8.2 EDL-SA Ground Rules and Assumptions

This section lists the Ground Rules and Assumptions (GR&A) as employed in the EDL-SA Study.

8.2.1 General Ground Rules and Assumptions

The ground rules and assumptions applicable to both robotic studies are

- Mass growth allowances and margins will be applied to all technologies and systems as described in Sect. 8.2.3.
- Subsystem performance parameters (e.g., engine Isp, engine T/W, vehicle inert mass fraction) are to be based upon historical data and trends.
- The atmosphere model used for this study will be MarsGRAM 2005.
- Turbulent flow onset will be estimated using the $Re_\theta = 200$ criterion. For $Re_\theta > 200$, the entire forebody will be considered to be turbulent.
- POST2 will be used for simulations.
- Representative guidance algorithms will be developed. Theoretical guidance algorithms will also be used.

- Vertical velocity at touchdown will be <= 1 m/s.
- On-orbit assembly will not be considered.
- Landed altitude capability will be a minimum of 0 km above MOLA.
- Landing site altitude sensitivities will be evaluated for -1 km MOLA to 2.5 km MOLA.
- Entry date: October 15, 2025.

8.2.2 Feed Forward Study Ground Rules & Assumptions

The following ground rules and assumptions are applicable to the Feed Forward Study. As the Feed Forward Mission DRM is intended to be a flight test of Exploration-class technologies, many of the ground rules and assumptions of the Exploration-class Study are included.

- Launch vehicle will be the Delta IV-H.
- Emphasis is given to those technologies that emerged from the Exploration-class Study as promising new technologies for landing 40 t of payload.
- Landed payload will be at least 2.0 t, constrained only by the capability of the Delta IV-H for the worst (highest arrival velocity) opportunity (2024) in the 2018–2028 time frame. [Note this assumption is changed from the original approved GR&A document]
- Separation events will be modeled on the basis of conceptual mechanical designs.
- Any shed drag device must never pass any closer than 1 km. to the target at any point in its trajectory ("keep-out zone" criterion).
- Simulations will include a method (e.g., divert maneuver, fly away) to ensure the "keep out zone" criterion is met.
- Aerocapture will be used to insert the vehicle into a 500 km apoapse orbit that will be circularized propulsively.
- Vehicle will be 3 axis stabilized
- Telecom is assumed to have body fixed antennas
- Back of lander has solar arrays
- HIADs are assumed to be rigid bodies
- Structure will be sized based on loads and will include plumbing, legs, guide rails, actuators, thruster placement
- System will assume sensor integration package (like MEDLI)
- Only the final configuration selected for packing analysis will receive ALHAT 6DOF characterization
- Subsystem performance parameters, e.g., engine Isp, engine T/W, inert mass fraction, will be based on historical data and trends.

8.2.3 Mass Growth Allowance and System Margin Policy

The design margins utilized in most previous Mars architecture/EDL studies have been quite optimistic. Indeed, some studies have carried no margin at all, and others have applied margins only to mass. The EDL-SA Study will use an integrated margin approach that is derived from current practice in the early phases of flight projects, e.g., development projects in the robotic missions in the Mars Program. This margin approach will provide an appropriate level of realism to the study results.

General Margin Policy

In developing mass estimates, three separate estimates should be provided. These are:

Current Best Estimate (CBE) Mass: This mass constitutes an assessment of the most recent baseline design including factors of safety or various knockdown factors. The estimate does not include any mass growth allowance.

Maximum Expected Value (MEV) Mass: This constitutes the CBE mass with the addition of mass growth allowance (MGA), where mass growth allowance consists of the predicted changes to the CBE based on an assessment of the design maturity.

MEV Mass = Current Best Estimate + Mass Growth Allowance

Allocated Mass: The allocated mass is the MEV mass with the addition of system margin.

Allocated Mass = MEV Mass + System Margin

The total mass growth allowance does not include any TRL-based augmentation.

Feed Forward Unique Margin Policy

The Feed Forward Study uses a baseline Mass Growth Allowance of 15%, based on the typical recommended range of 10–20% for designs at the layout stage given in AIAA S-120-2006.

The system dry mass margin is taken to be 30%, based upon the recommended value in GSFC-STD-1000E for a Pre-Phase A design.

8.2.4 Monte Carlo Parameters

The simulations used to perform system analyses in this study utilize Monte Carlo procedures to account for various uncertainties in the system and its environment. The uncertainties include both aleatory (variability) and epistemic (lack of knowledge) ones. We adopt the customary approach of describing the uncertainties by using probability density functions (PDFs). The PDFs represent the degree of belief about the distribution of the uncertain quantities—not only the nominal (most likely) values, but also their distribution between their plausible upper and lower limits. Of course, these subjective choices are informed by the statistical data that does exist and the team's experience with Monte Carlo simulations of previous Mars missions (Mars Exploration Rovers, Phoenix, MSL). Conservative adjustments were made because of lack of detailed information (experimental data, high-fidelity analyses) on current concepts. Table 7 and 8 list the parameters that are treated probabilistically in the MSL-I and the Feed Forward Studies, respectively. For each uncertain parameter, the rationale for the choice of distribution is included. The aerodynamic databases used in the simulations are based upon engineering-level tools. Multipliers on the aerodynamic coefficients model the uncertainties in these data. The model for the uncertainty in the Mars atmosphere is the model contained in MarsGRAM; the range for the random number seed is provided in the tables. Atmospheric density and wind perturbations are applied to all cases except the nominal.

Table 7. MSL-I Robotic Study Monte Carlo Parameters

Parameter	Nominal	Perturbation	Distribution	Rationale
Entry State Delivery and Knowledge Error	Position, Velocity as necessary to impact desired landing site.	Per Entry States File	Normal	Entry states file generated assuming a MSL DSN only attitude control system. Nominal entry state determined to be consistent with the Earth/Mars transfer trajectory and desired landing location for the date and time assumed.
Attitude Knowledge Error	Angle of Attack = 30deg. Bank = 70 deg.	0.25 deg about a varying rotation axis.	Direction of rotation axis computed uniformly in all directions (i.e. spherical distribution).	Again, a dsn only attitude control system is assumed.
Mass			Normal	
Angle of Attack (deg)	Case dependent	+/- 2	Normal	The nominal angle of attack will vary to achieve the desired nominal L/D. Perturbation value is typical variation from the ideal due to stability oscillations about the nominal trim angle.
Axial Force Coefficient Multiplier	-1	+/- 10 %	Normal	Larger than would be expected to provide sensitivity analysis. The sensitivity characteristics of the technology are important considerations. Also the aerodynamics are uncorrelated, to further magnify the sensitivities. Many technologies will look good at their design point – one major discriminator will be sensitivity.
Normal Force Coefficient multiplier	1	+/- 10 %	Normal	See Axial Force Coefficient Multiplier discussion.
Atm Random #	1	1-29999	Integer Uniform	This is used by the atmosphere program to determine the variability in the density and wind profiles. The range is that allowed by the Mars atmosphere program used in the simulation. Also, other atmospheric parameters have been set, based on MSL experience, that would further stress the system.
Dusttau	0.7	0.1:0.9	Uniform	This determines the dust loading and thus the density and wind profiles that the vehicle will experience. This range provides large variability, but would not include dust storms.

Table 8. Feed Forward Robotic Study Monte Carlo Parameters

Parameter	Nominal	Perturbation	Distribution	Rationale
Mass Variation (kg)	0	+/- 100	Normal	Not currently used – Sensitivity to ballistic coefficient needs to be quantified as the study matures – i.e. those technologies with less sensitivity would be favored over those with a high sensitivity. (also this sensitivity will be nonlinear in many instances). To minimize the number of Monte Carlo scripts that must be certified, this capability has already been added – but will not be exercised until later in the study.
Axial Force Coefficient Multiplier	-1	+/- 10 %	Normal	Larger than would be expected to provide sensitivity analysis. The sensitivity characteristics of the technology are important considerations. Also the aerodynamics are uncorrelated, to further magnify the sensitivities. Many technologies will look good at their design point – one major discriminator will be sensitivity.
Normal Force Coefficient multiplier	1	+/- 10 %	Normal	See Axial Force Coefficient Multiplier discussion.
Atm Random #	1	1-29999	Integer Uniform	This is used by the atmosphere program to determine the variability in the density and wind profiles. The range is that allowed by the Mars atmosphere program used in the simulation. Also, other atmospheric parameters have been set, based on MSL experience, that would further stress the system.
Dusttau		0.1:0.9	Uniform	This determines the dust loading and thus the density and wind profiles that the vehicle will experience. This range provides large variability, but would not include dust storms.

8.3 Evaluation Criteria

The Feed Forward Robotic Study will use the following strategy for selecting an optimal Feed Forward system design.

The nominal DRM for the FF study is described in section 8.1. The strategy for selecting an optimal design will include a three-step process. Step 1 will be to select the controller based on 6 DOF aerocapture simulations. Three controllers will be considered: y and z center of gravity (cg) control, bank angle control and a cg and bank combination controller, henceforth known simply as the combo controller. The controller will be selected based on the minimum number of failed (outlying) aerocapture trajectories, the maximum corridor width and ease of physical implementation. None of the control

methods have been employed on vehicles of this size. Several detailed configurations will be generated to ensure that the vehicle does allow for the control authority required to adequately land the vehicle at the specified location.

The second step will use the control method selected from Step 1. Step 2 will use the 6DOF aerocapture simulation and a 3 DOF entry simulation to determine which type of TPS material to be used on the aerocapture HIAD by considering HIAD size, controllability and packaging. The options include the insulator (case already set up from step 1) and the ablator. The trade will compare the potential reduction in development cost using the insulator because the same design potentially can be used for the entry HIAD compared to the advantage of packaging and controlling a smaller ablative TPS HIAD for aerocapture.

The third and final step in the Feed Forward selection process will be to trade the configuration determined in Step 2 using the control method selected in Step 1 and trade the use of one dual use HIAD for aerocapture and entry versus using a two HIAD system (one larger HIAD for aerocapture and a smaller one for entry). In conjunction with Step 3 of the design selection process, detailed packaging analysis will be performed so that approximations of the inertias can be incorporated into both a 6DOF aerocapture and entry simulation. The goal of the design is to illustrate detailed packaging arrangements, ensure that the inertias are stable and that 6DOF system closes while providing maximum landed payload to the surface of Mars.

The ALHAT sensor suite will be included only in the final Feed Forward design configuration. Sensor operation ranges will be determined using the 6DOF entry simulation. The results will be provided to the ALHAT team.

In summary, the down select process for the Feed Forward effort involves five simulations, which are shown in Table 9.

Table 9. Feed Forward TPS and Control Method Options

Design	NOM	A	B	C	D
AC TPS	Insulator	Insulator	Insulator	Ablator	Nom, A, B or C
Entry TPS	Insulator	Insulator	Insulator	Insulator	
Ctrl Method	CG	Bank	Combo	Nom or A or B	Nom or A or B

8.4 Feed Forward Study Products

The high-level products expected by the EDL-SA funders, as approved by CCRB and TISC decisions, are listed in Table 10.

Table 10. High-level Products for FF Study

Maximum payload the Delta IV-H can deliver
Required performance of supersonic retro-propulsion system
Next level of detail on packaging, mass properties, transitions, structures, propulsion, etc
Optimum material/TPS, L/D, and size of the HIAD for aerocapture and entry
Determine if active cg control provides benefits over the use of bank only
Determine the sensor performance ranges for an ALHAT like navigation & sensor system at Mars

It is expected that a final Technical Memorandum (TM), or similar, will be generated that will document a summary of all the products discussed above.

Appendix B - EDL Technology Needs

Category	Technology	TDP Objective-EDLSA Exploration Class Missions (Year 1)	Mars EDL Rationale	Refinements from EDLSA Exploration Feed Forward Study (Year 2)
Sub-Scale Component Analysis, Testing & Evaluation				
Aeroshell/TPS Design and Dev	Rigid Aeroshell Tools	Develop, calibrate and validate tools & processes for generating aero/aerothermal databases with credible uncertainty estimates for slender rigid entry/aerocapture vehicles. Builds on existing low TRL (1-3) R&D program in ARMD.	Lower uncertainty aero/aerothermal database tools enable margin reduction for rigid aeroshells	Use software configuration control mechanisms for better productivity and verifiability
Aeroshell/TPS Design and Dev	Dual Heat-Pulse TPS	Maturation of rigid, dual heat-pulse TPS capable of Mars aerocapture, cool down in orbit, and subsequent entry with a single aeroshell	Enables single heat shield (and structure) for aerocapture & entry, resulting in lower mass and cost	No refinements identified
Aeroshell/TPS Design and Dev	Rigid Aeroshell Vehicle Design Studies	Design and test rigid aeroshell shapes for aerodynamic performance and controllability for Mars aerocapture and entry. Perform pre-Phase A design for packaging, structures, and mechanisms in order to assemble Manufacturing Development Units.	Trade studies and pre-Phase A design activities are necessary to ensure technology viability and to assess mass, volume and design maturation	Consider size, shape and mass optimization based on new knowledge that potential Mars Payloads will be significantly shorter than assumed for DRA5 (i.e. 10x13 m rather than 10x30 m). Also need to fully examine all transition maneuvers.
SS Retro-Prop Dev	Supersonic Retro-Propulsion	Assess range of feasibility of using propulsion for supersonic deceleration for Exploration scale missions, considering multiple nozzle configurations and locations along with representative vehicle configurations	**Supersonic deceleration** is a key technology gap, that **appears to have a single-point technology solution—Supersonic Retropulsion—for landing large payloads on Mars**. Aerodynamic decelerators do not meet the supersonic deceleration requirements of Exploration-class missions.	**Recommend to accelerate SRP development to a point that feasibility has been demonstrated ASAP**
Deployable/Inflt Decel Dev	Flexible Aeroshell Tools	Develop, calibrate and validate tools & processes for generating aero/aerothermal databases with credible uncertainty estimates for flexible entry/aerocapture vehicles, including aeroelastic effects. Builds on existing low TRL (1-3) R&D program in ARMD.	Lower uncertainty aero/aerothermal database tools enable margin reduction for flexible aeroshells; existing methods are immature compared to the rigid case. Flight dynamics knowledge required to determine controllability issues & evaluate solutions.	Include tools for rigid deployables not covered in Rigid Aeroshell Tools. Consider alternate modes (e.g. cg/RCS control, shape control) of guidance and control. Utilize software configuration control mechanisms for better productivity and verifiability
Deployable/Inflt Decel Dev	Deployable, Flexible Materials	Maturation of deployable (rigid and flexible) materials (high-temperature heatshield, insulation, and structures; flexible ablators; dual use systems) capable of Mars aerocapture and entry	Required for Deployable (Rigid and Flexible) Aerodynamic Decelerators	Consider size, shape and mass optimization and effect of charring
Deployable/Inflt Decel Dev	Flexible Aeroshell Vehicle Design Studies	Design and test deployable/inflatable (rigid and flexible) aeroshell shapes for aerodynamic performance, structural strength and controllability for Mars aerocapture and entry. Perform pre-Phase A design for packaging, structures, and mechanisms in order to assemble Manufacturing Development Units.	Trade studies to select optimum deployable (rigid and inflatable) aeroshell shapes, materials and control surface/RCS systems are necessary	Investigate the ability to perform and model HIAD separation from the payload. Include all known dynamical effects including flexible joint interaction

GN&C	Autonomous Precision Navigation with Hazard Avoidance	Develop sensors, navigation and controls systems for precision landings with hazard avoidance on Mars.	This is in the current ETDD Program but is focused on lunar landings. The same technology will be needed at Mars, albeit with somewhat different requirements.	Additional insight into performance requirements was gained, but no fundamentally new objectives were identified
Aerocapture Dev	Aerocapture Development	Establish requirements for an Aerocapture Technology Validation Flight Test, to provide system-level validation of blunt-body aerocapture applicable to Mars, Earth, Titan, and Venus	Aerocapture reduces number of Ares V launches for Exploration-class missions from 11 to 7	Consider ability to jettison drag device after aerocapture pass but while in sensible atmosphere. Investigate torques caused by aero/RCS interactions. Double the usual aerodynamic uncertainties in systems analyses to account for flexibility effects.
Sub-Scale System Testing				
	Supersonic Retro-Propulsion Flight Test Program	Flight demonstration (TRL=6) of controllability of supersonic retro-propulsion descent system. A sounding rocket or a balloon will suffice. Includes funds for a second flight unit.	Supersonic deceleration is a key technology gap, that appears to be a single-point technology need for landing large payload on Mars. Aerodynamic decelerators do not meet the supersonic deceleration requirements of Exploration-class missions.	Consider developing a dedicated reusable testbed to test critical EDL technologies and flight instrumentation
	Deployable/Inflatable Decelerator Flight Test Program	Flight demonstration (TRL=6) of Deployable, Inflatable Aerodynamic Decelerator. Includes funds for a second flight unit.	Enables lower ballistic entries for Exploration-class missions, increasing timeline margin, and permits decoupled tailoring of decelerator and payload. Simulation results indicate a savings of 40 mT in Mars arrival Mars compared with a rigid aeroshell.	Consider developing a dedicated reusable testbed to test critical EDL technologies and flight instrumentation
	Aerocapture Flight Test	Flight demonstration (TRL=6–7) of Aerocapture in upper Earth's atmosphere	Aerocapture reduces number of Ares V launches for Exploration-class missions from 11 to 7	No refinements identified
Full-Scale System Testing				
	Feed-Forward Technology Mars Flight Test	Not addressed in Year 1	Flight demonstration (TRL=8) of EFF technologies at Mars with useful Exploration payload in the 2.5–3 t range.	Use technologies from EDL-SA (or future studies) EFF robotic mission design—currently, aerocapture and entry with HIADs (single or dual), descent and landing with propulsion (cost does not include payload)

Appendix C - HIAD Diameter Trade Study Results

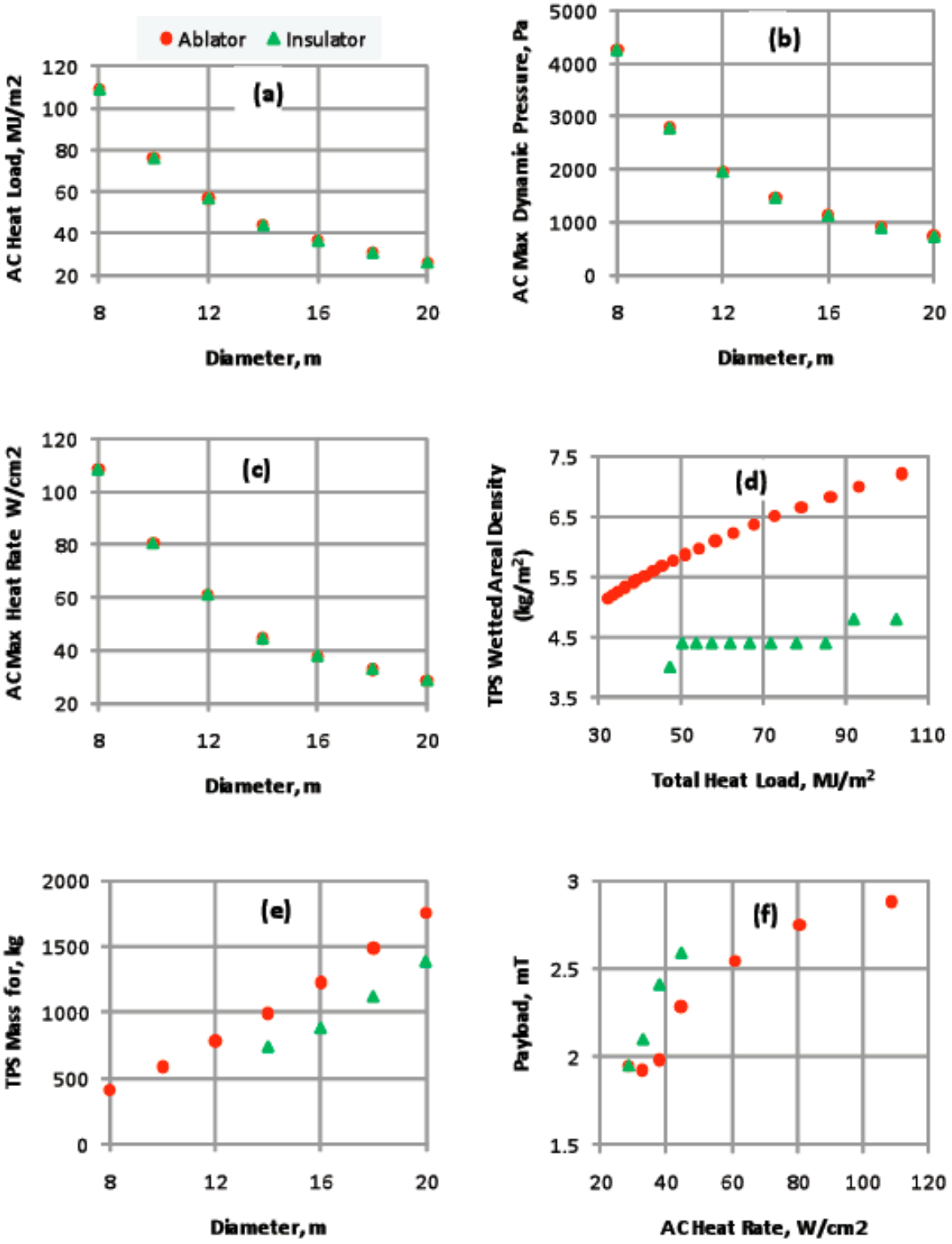

Figure C-19. Mass Model Trade for Single HIAD Concept (EFF-2)

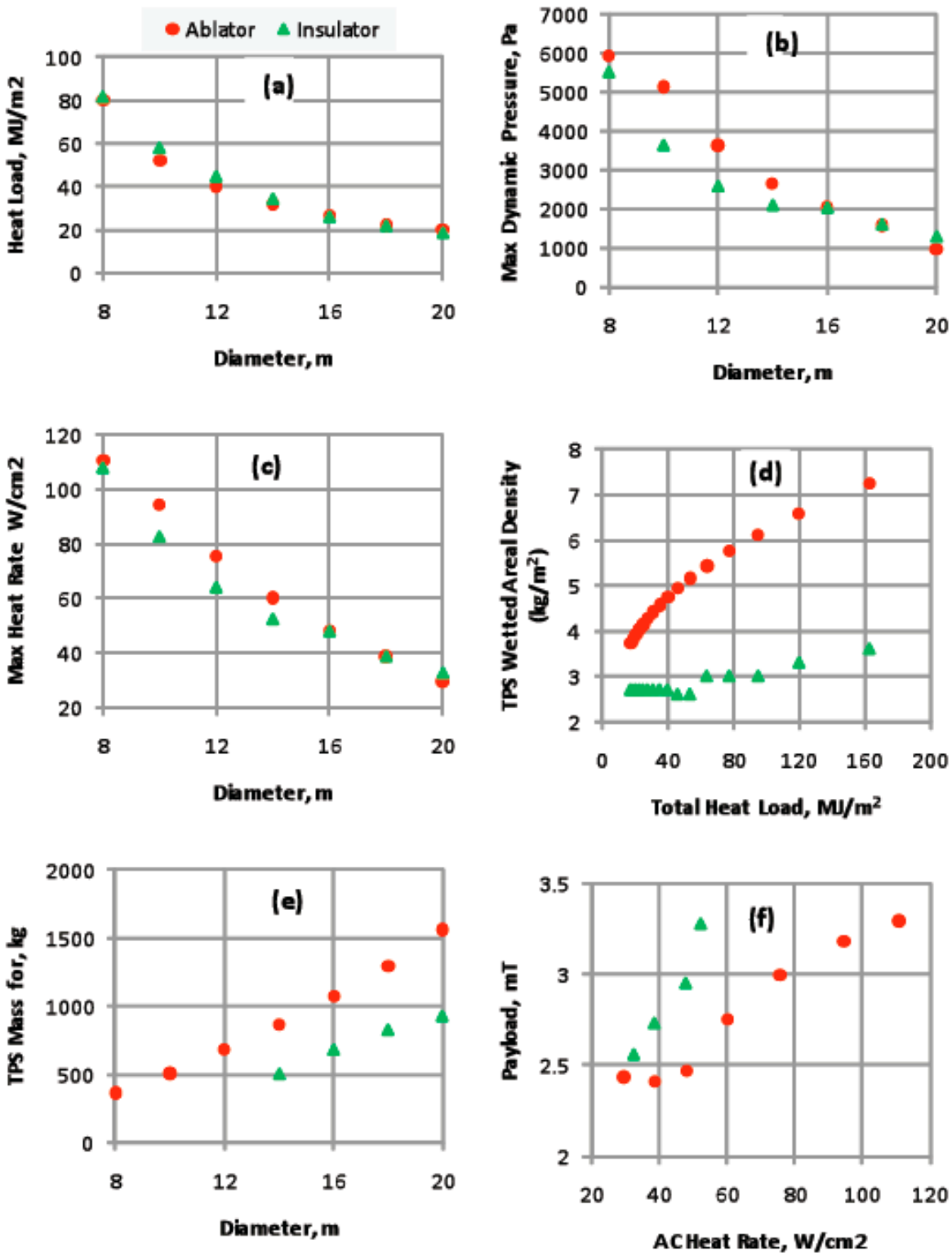

Figure C-20. Mass Model Trade for Direct Entry Concept (EFF-3)

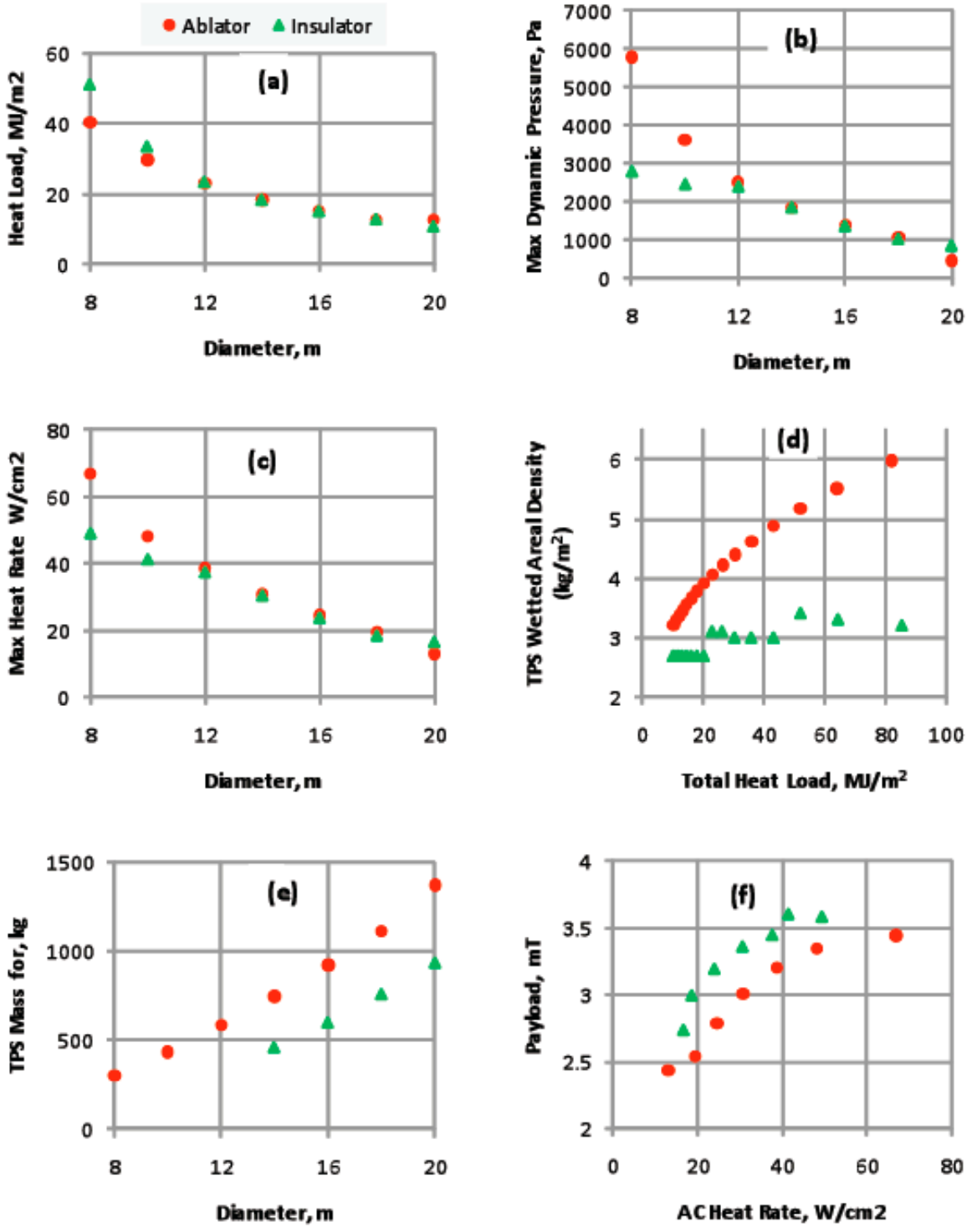

Figure C-21. Mass Model Trade for Direct Entry Concept (EFF-4)

Appendix D - Simulation Monte Carlo Dispersions

Parameter	Nominal Value	Dispersion	Units	Distribution
Initial State				
Entry Flight Path Angle	**Guidance Dependent**	**+/- 0.25**	**deg**	**Normal**
Hyperbolic Velocity	**5463.59**	**+/- 20**	**m/s**	**Normal**
B-plane Angle	**270.0**	**+/- 0.1**	**deg**	**Normal**
Time of Flight	**-30.0**	**+/- 2.0**	**sec**	**Normal**
Atmospheric Uncertainties				
Dust Tau	**0.45**	**0.1 to 0.9**	**[nd]**	**Uniform**
Perturbation Seed Number	**1**	**1 to 29999**	**[nd]**	**Integer**
Density Multiplier	**1.0**	**+/- 15%**	**[nd]**	**Uniform**
Initial Attitude and Rate Uncertainties				
Alpha	**-7 for L/D 0.10 -18.0 for L/D 0.25**	**+/- 0.25**	**deg**	**Normal**
Beta	**0.0**	**+/- 0.25**	**deg**	**Normal**
Bank Angle	**0.0**	**+/- 0.25**	**deg**	**Normal**
Roll Rate $_{BODY}$	**0.0**	**+/- 0.10**	**deg/s**	**Normal**
Pitch Rate $_{BODY}$	**0.0**	**+/- 0.10**	**deg/s**	**Normal**
Yaw Rate $_{BODY}$	**0.0**	**+/- 0.10**	**deg/s**	**Normal**
Aerodynamic Uncertainties				
CA Multiplier	**1.0**	**0.9:1.1**	**[nd]**	**Normal**
CN Multiplier	**1.0**	**0.9:1.1**	**[nd]**	**Normal**
CY Multiplier	**1.0**	**0.9:1.1**	**[nd]**	**Normal**
Mass Property Uncertainties				

Appendix E - Simulation Monte Carlo Navigation and Sensor Dispersions

Parameter						*Dispersion*		
		Mean	**Units**			**3-sigma**	**Units**	**Type**
Sensors								
Accelerometer*	bias	0	m/s^2	+/-		8.250E-04	m/s^2	Gaussian
(same error for each direction)	scale factor	0	%	+/-		4.500E-04	%	Gaussian
	random noise		m/s^2	+/-		9.000E-05	m/s^2	Gaussian
Gyro*	bias	0	rad/s	+/-		1.745E-07	rad/s	Gaussian
(same error for each direction)	scale factor	0	%	+/-		2.700E-05	%	Gaussian
	random noise		rad/s	+/-		1.309E-07	rad/s	Gaussian
Startracker*	bias	0	deg	+/-		0.01667	deg	Gaussian
(same error for each direction)	random noise	0	deg	+/-		0.04167	deg	Gaussian
Altimeter	bias	0	m	+/-		0.0	m	Gaussian
	scale factor	0	%	+/-		0.0	%	Gaussian
	random noise		m	+/- +/-		15.000	m	Gaussian
Velocimeter (lo-fi)	bias	0	m/s	+/-		0.003	m/s	Gaussian
	scale factor	0	%	+/-		0.000	%	Gaussian
	random noise		m/s	+/-		0.018	m/s	Gaussian
TRN	bias	0	m/s	+/-		15.000	m	Gaussian
TRN	random noise		m	+/- +/- +/-		24.7 (12–15km) 0.3225% alt – 14.025 (7–12 km) 8.55 (5–7 km)	m	Gaussian
Initial States								
NAV States	inertial position error		km	+/- +/- +/- +/-		2.0 (xi) 2.0 (yi) 2.0 (zi)	km	Gaussian
	inertial velocity error		m/s	+/- +/-		2.0 (vxi) 2.0 (vyi) 2.0 (vzi)	m/s	Gaussian
	attitude error		deg	+/-		0.04	deg	Gaussian

***Monte Carlo run with IMU/startracker error only since ALHAT navigation filter**

REPORT DOCUMENTATION PAGE

Form Approved
OMB No. 0704-0188

1. REPORT DATE *(DD-MM-YYYY)*	2. REPORT TYPE	3. DATES COVERED *(From - To)*
01- 02 - 2011	Technical Memorandum	

4. TITLE AND SUBTITLE

Entry, Descent and Landing Systems Analysis Study: Phase 2 Report on Exploration Feed-Forward Systems

5a. CONTRACT NUMBER

5b. GRANT NUMBER

5c. PROGRAM ELEMENT NUMBER

6. AUTHOR(S)

Dwyer Cianciolo, Alicia M.; Davis, Jody L.; Engelund, Walter C.; Komar, D. R.; Queen, Eric M.; Samareh, Jamshid A.; Way, David W.; Zang, Thomas A.; Murch, Jeff G.; Krizan, Shawn A.; Olds, Aaron D.; Powell, Richard W.; Shidner, Jeremy D.; Kinney, David J.; McGuire, M. Kathleen; Arnold, James O.; Covington, M. Alan; Sostaric, Ronald R.; Zumwalt, Carlie H.; Llama, Eduardo G.

5d. PROJECT NUMBER

5e. TASK NUMBER

5f. WORK UNIT NUMBER

892840.01.07.10

7. PERFORMING ORGANIZATION NAME(S) AND ADDRESS(ES)

NASA Langley Research Center
Hampton, VA 23681-2199

8. PERFORMING ORGANIZATION REPORT NUMBER

L-19969

9. SPONSORING/MONITORING AGENCY NAME(S) AND ADDRESS(ES)

National Aeronautics and Space Administration
Washington, DC 20546-0001

10. SPONSOR/MONITOR'S ACRONYM(S)

NASA

11. SPONSOR/MONITOR'S REPORT NUMBER(S)

NASA/TM-2011-217055

12. DISTRIBUTION/AVAILABILITY STATEMENT

Unclassified - Unlimited
Subject Category 18
Availability: NASA CASI (443) 757-5802

13. SUPPLEMENTARY NOTES

14. ABSTRACT

NASA senior management commissioned the Entry, Descent and Landing Systems Analysis (EDL-SA) Study in 2008 to identify and roadmap the Entry, Descent and Landing (EDL) technology investments that the agency needed to successfully land large payloads at Mars for both robotic and human-scale missions. Year 1 of the study focused on technologies required for Exploration-class missions to land payloads of 10 to 50 t. Inflatable decelerators, rigid aeroshell and supersonic retro-propulsion emerged as the top candidate technologies. In Year 2 of the study, low TRL technologies identified in Year 1, inflatables aeroshells and supersonic retropropulsion, were combined to create a demonstration precursor robotic mission. This part of the EDL-SA Year 2 effort, called Exploration Feed Forward (EFF), took much of the systems analysis simulation and component model development from Year 1 to the next level of detail.

15. SUBJECT TERMS

Systems analysis; Entry; Descent; Landing; Exploration; Mars; Technology

16. SECURITY CLASSIFICATION OF:			17. LIMITATION OF ABSTRACT	18. NUMBER OF PAGES	19a. NAME OF RESPONSIBLE PERSON
a. REPORT	b. ABSTRACT	c. THIS PAGE			STI Help Desk (email: help@sti.nasa.gov)
					19b. TELEPHONE NUMBER *(Include area code)*
U	U	U	UU	53	(443) 757-5802